

Distribution Agreement

In presenting this thesis or dissertation as a partial fulfillment of the requirements for an advanced degree from Emory University, I hereby grant to Emory University and its agents the non-exclusive license to archive, make accessible, and display my thesis or dissertation in whole or in part in all forms of media, now or hereafter known, including display on the world wide web. I understand that I may select some access restrictions as part of the online submission of this thesis or dissertation. I retain all ownership rights to the copyright of the thesis or dissertation. I also retain the right to use in future works (such as articles or books) all or part of this thesis or dissertation.

Signature:

Rebecca C. Roffman

Date

Synaptic strength in the leech heartbeat central pattern generator: Animal to animal
variability and stereotypy

By

Rebecca Roffman
Master of Science
Neuroscience

Ronald L. Calabrese, Ph.D.
Advisor

Shawn Hochman, Ph.D.
Committee Member

Astrid Prinz, Ph.D.
Committee Member

Pete Wenner, Ph.D.
Committee Member

Accepted:

Lisa A. Tedesco, Ph.D.
Dean of the James T. Laney School of Graduate Studies

Date

Synaptic strength in the leech heartbeat central pattern generator: Animal-to-animal
variability and stereotypy

By

Rebecca C. Roffman
B.S, Union College, 2004

Advisor: Ronald L. Calabrese, Ph.D.

An abstract of
A thesis submitted to the Faculty of the
James T. Laney School of Graduate Studies of Emory University
in partial fulfillment of the requirements for the degree of
Master of Science
in Neuroscience
2011

Abstract

Synaptic strength in the leech heartbeat central pattern generator: Animal-to-animal variability and stereotypy

By Rebecca C. Roffman

This study seeks to characterize, as quantitatively as possible, the strength of each synapse within the leech heartbeat central pattern generator and to examine the animal-to-animal variability and stereotypy that can underlie a circuit whose output is functionally stable. A central pattern generating circuit (CPG) that produces a reliable, stereotyped output in isolation is an excellent candidate for the study of the inner-workings of neural networks. The use of invertebrates is advantageous because of the small number and large size of constituent neurons, and their identifiability.

The importance of both intrinsic properties of neurons and their synaptic interactions in shaping network output has been well illustrated. Intrinsic properties not only shape activity and response properties of the neurons, but ion channel expression can vary 2-5 fold across preparations in the same identifiable cell, while the network continues to produce a stereotyped behavioral output (Schulz, Goaillard et al. 2006). Modeling studies have suggested that both intrinsic properties and synaptic strengths within a network can vary substantially while maintaining a stable output (Prinz, Bucher et al. 2004).

The leech heartbeat CPG is a small network responsible for blood flow within a closed circulatory system including two parallel heart tubes in the medicinal leech. The CPG is composed of 7 bilateral pairs of heart interneurons connected via both inhibitory chemical synapses and electrical junctions that give rise to a functionally stable, rhythmic output. Each of the 15 synapses within the core central pattern generator was measured for synaptic strength across a minimum of 7 individuals and the variability was calculated. Synaptic strengths within the leech heartbeat central pattern generator varied 3 to 14 fold between individuals (depending on the specific synapse). The balance between multiple inputs onto various postsynaptic targets was explored. Of the 5 comparisons made within the core CPG two showed a clear maintenance of synaptic strength ratios while the other three showed no such relationship. We conclude that the leech heartbeat central pattern generator can withstand tremendous variability in synaptic strengths despite a relatively stable circuit output. The network clearly preserves the relationship of several different inputs despite tremendous variability.

Synaptic strength in the leech heartbeat central pattern generator: Animal-to-animal
variability and stereotypy

By

Rebecca C. Roffman
B.S. Union College, 2004

Advisor: Ronald L. Calabrese, Ph.D.

A thesis submitted to the Faculty of the
James T. Laney School of Graduate Studies of Emory University
in partial fulfillment of the requirements for the degree of
Master of Science
In Neuroscience

2011

Table of Contents:

Introduction.....1
Methods.....9
Results.....13
Discussion.....26
Figure Legends.....34
References.....42

Figures:

Figure One.....45
Figure Two.....46
Figure Three.....47
Figure Four.....48
Figure Five.....49
Figure Six.....50
Figure Seven.....51
Figure Eight.....52
Figure Nine.....53
Figure Ten.....54
Figure Eleven.....55

Introduction

Variability in Neural Networks: Using Invertebrates

A central pattern generating circuit (CPG) is an excellent candidate for study of the inner-workings of networks because of its ability to produce fictive motor patterns in isolation, which are both stereotyped and temporally complex (Selverston 2010). Examples of central pattern generating networks include those that control locomotion, breathing, and chewing (Lund and Kolta 2006; Kiehn, Dougherty et al. 2010)). These networks are ubiquitous across phyla. CPGs involved in motor pattern production have been well studied for decades with regards to both individual network components and neuromodulation (Dickinson 2006) (Katz 1998).

The identifiability of these CPG neurons, with characteristic properties and connections, presents a good opportunity to study in detail the connections between groups of neurons that come together to produce specific behavioral outputs. Because of these technical advantages, rapid progress has been made in the field, and we are now able to ask more detailed and complex questions. More specifically, the use of invertebrates is advantageous because of the small number and large size of constituent neurons, and their identifiability. Work with invertebrate CPGs provides us with insights that are generally applicable to normal CPG and general network function (Grillner, Markham et al. 2005; Marder, Bucher et al. 2005). Understanding how these smaller circuits work will allow us to understand the reaction of CPGs in vertebrates to spinal cord injury and disease. This work also helps to contribute to the general understanding of the dynamics and functioning of neural networks.

Tremendous progress has been made in understanding network dynamics and

synaptic interactions through work in CPGs. Previous work in the stomatogastric nervous system (STNS) of crustaceans has illustrated the importance of the synaptic connections between network components. This work has illuminated how inhibitory inputs and electrical coupling can interact within the circuit, and the importance of short-term dynamics in achieving phase relationships among the CPG elements (Mamiya and Nadim 2005; Rabbah and Nadim 2005). It is important to continue this work in a system where the CPG is composed of interneurons, as well as a CPG that is segmentally distributed and relies on spike-mediated synaptic transmission, much like in vertebrate systems. Also of interest is an analysis of a central pattern generating network with multiple flexible phase relationships, similar to the vertebrate locomotor CPGs (Mentel, Cangiano et al. 2008).

A recent body of work has begun to explore animal-to-animal variability in both network output as well as within the network components. The output of the pyloric CPG of crustaceans is highly stereotyped in both cycle period and phase relations (Bucher, Prinz et al. 2005; Bucher, Taylor et al. 2006). The intrinsic properties that underlie this stereotypy, however, have been shown to be highly variable across animals. In the stomatogastric nervous system, maximal potassium channel conductances vary over a two to five fold range without any qualitative change in network output (Schulz, Goaillard et al. 2006; Schulz, Goaillard et al. 2007). This variability in maximal conductances has been directly correlated to levels of gene expression for the channel. Other examples of this animal-to-animal variability in intrinsic properties without concomitant changes in activity have been noted in both the crustacean STNS, and the Purkinje cells of the rat cerebellum (Swensen and Bean 2003; Swensen and Bean 2005).

Based on this data and work in the leech heartbeat system from our own lab, Marder and Goaillard, in a recent review, proposed that synaptic strength (maximal conductances) also varies two-to-four-fold between individuals without any remarkable changes in activity (Marder and Goaillard 2006).

Similarly, modeling work in the crustacean STNS has suggested that a wide variety of parameter sets can give rise to qualitatively similar networks within the bounds of the previously mentioned biological variability (Prinz, Bucher et al. 2004). Theoretical work emphasizes that the underlying state of neural networks that produce these qualitatively similar outputs can be quite different, however, such that they respond to parameter changes very differently (Goldman, Golowasch et al. 2001).

Given all of this information on the prevalence and importance of animal-to-animal variability in both intrinsic properties and synaptic strengths in central pattern generating networks, it became very important to document this variability in other systems, and ultimately to understand the implications of this variability for the operation and modulation of CPGs and neural networks in general. A full survey of network synapses and interactions within a single CPG may illuminate how these important interactions and balances affect the circuit.

The Leech Heartbeat Central Pattern Generator

The leech is a segmented worm, and this organization is evident in the underlying organ and nervous systems. The circulatory system of the leech consists of blood flow through a closed system with two parallel heart tubes (Thompson and Stent 1976a; Krahl and Zerbst-Boroffka 1983; Wenning, Cymbalyuk et al. 2004). Rhythmic constriction of

the two heart tubes drives circulation in the network (Boroffka and Hamp 1969), (Thompson and Stent 1976a). These muscle contractions are entrained by the rhythmic motor output of the heartbeat central pattern generator (Maranto and Calabrese 1984).

The heartbeat pattern (beat period of 4-10 seconds) is asymmetric, with one heart, the peristaltic heart, constricting with a rear-to-front progression and high systolic pressure to push blood forward along its length. The other heart, the synchronous heart, constricts nearly synchronously with low systolic pressure and pushes blood into the periphery as well as supporting a rearward flow (Wenning and Meyer 2007). The hearts undergo regular, precipitous switches in roles every 20-40 heartbeats.

The central nervous system of the leech is comprised of 21 mid-body ganglia linked by nerve bundles called connectives. At either end of this chain are fused ganglia known as “brains.” Each ganglion contains approximately 400 neurons (Macagno 1980) most of which are bilaterally paired and repeated from ganglion to ganglion. The ganglia are sufficiently stereotyped such that it is possible to reliably identify the same neuron between ganglia and in different individuals by its location, soma size, and characteristic electrical activity.

The underlying neural network is a small, well-studied central pattern generator consisting of interneurons that output onto segmental motor neurons responsible for the constriction of the heart tubes (Calabrese 1977). The core central pattern generator has seven identified pairs of well studied heart (HN) interneurons, located in each segmental ganglion numbers one through seven (indexed by ganglion number and body side HN(L,1) to HN(R,7))(Fig. 1 – this excludes the unidentified cell HN(X).) These oscillatory heart interneurons interact synaptically among themselves through both

chemical inhibitory synapses and electrical junctions. Recently two more pairs of premotor interneurons (rear premotor interneurons) have been identified in ganglia 15 and 16; these neurons do not feedback onto the CPG core network and are not further considered here (Wenning, Norris et al. 2008).

The timing circuit of the leech heartbeat CPG provides oscillatory drive to the rest of the network. All four pairs of interneurons in this circuit have the ability to reset and entrain the heartbeat rhythm (Peterson and Calabrese 1982). This circuit contains the heart interneurons located in ganglia 1 and 2, known as the coordinating interneurons as well as the heart interneurons located in ganglia 3 and 4, known as the oscillator interneurons.

Side-to-side coordination in the network is established through reciprocal inhibitory connections between the bilaterally paired oscillator interneurons located in ganglia 3 and 4. Each of these pairs forms a half-center oscillator through reciprocal inhibition, which then drives the rhythmic bursting of the network through posterior-going synaptic connections (Calabrese 1977). These oscillator interneurons are also known as the front premotor interneurons, as they provide the output to the motor neurons that are the output of the CPG. Each reciprocal inhibitory pair of oscillator interneurons within a ganglion is linked via an ipsilateral electrical connection. There is evidence that this is a strong connection (Thompson and Stent 1976c), although systematic measurements have not previously been made.

The coordinating interneurons located in ganglia 1 and 2 send inhibitory connections down the nerve cord to the oscillator interneurons in ganglia 3 and 4, and provide the important inputs for coordinating the bursting in the two half-center

oscillators. These coordinating interneurons couple the oscillations of the HN(3) and HN(4) interneurons thereby guaranteeing that a coherent time signal is sent to the rest of the heartbeat network. The coordinating interneurons can play this coupling role because they have spike initiation zones in the 3rd and 4th ganglia, and have input from and output connections onto the HN(3) and HN(4) interneuron pairs (Masino and Calabrese 2002).

The oscillator interneurons in ganglia 3 and 4 also send inhibitory synapses down the nerve cord onto the heart interneuron in ganglion 5, known as the switch (HN(5)) interneuron. The activity of the switch interneuron is directly correlated to changes in coordination mode within the circuit (Gramoll, Schmidt et al. 1994). This cell can be either silent or rhythmically active and the activity state of the cell determines whether the ipsilateral heart will be in the peristaltic or synchronous coordination mode. When the switch interneuron is active, the ipsilateral side is in the synchronous mode and when it is inactive, the ipsilateral side is in the peristaltic mode (Gramoll, Schmidt et al. 1994). The cells undergo regular, precipitous, reciprocal switches in activity state every twenty to forty cycles (one-hundred to four-hundred seconds).

The switch interneurons are extremely important to the circuit, because they are causing the critical switch in coordination mode of the heart tubes by shifting the phasing of the middle premotor interneurons (HN(6) and HN(7)) with respect to the timing network. This relative timing is important in providing coordination mode information. Inputs onto these interneurons are extremely important to the output of the network because they are the only way for the switch interneurons to be coordinated with the bursting of the timing network.

The patterning circuit is composed of the four middle premotor interneurons, located in ganglia 6 and 7. These are purely premotor cells that provide synaptic input to more rearward heart motor neurons all the way along the nerve cord to ganglion 18 (Norris, Weaver et al. 2006). When one heart is in the peristaltic coordination mode, there is a rear to front progression of bursting, with the middle premotor interneurons leading the oscillator interneurons on that side while on the other side the heart is in the synchronous mode and there is a near synchronous bursting of the middle premotor interneurons and the oscillator interneurons. Switches in coordination mode result from side-to-side shifts in the phasing of the middle premotor interneurons.

The middle premotor interneurons receive inhibitory synaptic connections from both HN(5) switch interneurons. This bilateral connection is the only example of such in the leech heartbeat central pattern generator, and it allows for the important phasing information provided by either of the HN(5) switch interneurons to be relayed to the middle premotor interneurons on both sides and therefore affect the motor output of the CPG bilaterally. The middle premotor interneurons also receive an electrical connection from the oscillator interneurons in ganglia 3 and 4. This electrical connection causes the middle premotor interneurons on the two sides to fire slightly out of phase despite bilateral inhibitory input from the single active switch interneuron.

Animal-to-animal variability in the phasing of the leech heartbeat CPG is relatively small (Norris, Weaver et al. 2006). Based on this small variability, it appears that the exact phase relationships between network components are critical. How then, is phase maintained in the face of variability of intrinsic properties, strength of interneuronal connections, and strength of output connections?

The output of the heartbeat CPG onto the segmental motor neurons has been well studied (Norris, Weaver et al. 2007). The strength of the synaptic connections from premotor interneurons to heart motor neurons is highly variable over a two to five-fold range. This connection strength does not change with switches in coordination mode. Despite this variability in individual synaptic strength, relative synaptic strength within preparations was less variable. This is evident from examination of the characteristic intersegmental profile of connection strengths, which illustrates that relative synaptic strength, though not strictly maintained for these synapses across individuals, shows clear trends (Norris, Weaver et al. 2007).

Maintenance of Synaptic Strength Ratios: How can a network tolerate a high degree of variability in synaptic strengths?

A network neuron receives numerous inputs (excitatory, inhibitory and modulatory) and the neuron must integrate all of these inputs to produce the appropriate activity. Logic would dictate that certain synapses within the network have a higher functional impact and importance than others, and therefore the maintenance of their strengths and the balance between these inputs would be maintained in the face of high variability. Without any maintenance of relative strengths it would be difficult to believe that the synaptic interactions between the network neurons are critical in the shaping of network output.

How important is maintaining the balance of synaptic strength in the functional output of a neuronal circuit?

This study seeks to answer the question of if the synaptic strengths that underlie a functionally stable circuit output can vary between individuals (and to what extent). To address this question, we conducted a sequence of experiments that measured the synaptic strength and individual variability in the synapses of the leech heartbeat central pattern generator. Are the various connections in a central pattern generator balanced regardless of their general size? To address this question we compared relative strengths at several key points within the network in an attempt to understand the balance of synaptic and electrical inputs onto a postsynaptic target.

Materials and Methods:

Animals and Solutions

Leeches (*Hirudo sp*) (Siddal, Trontelj et al. 2007) were obtained from commercial suppliers (Leeches USA, Westbury, NY and Biopharm, Charleston, NC) and maintained in artificial pond water at 15°C. After the animals were anesthetized in cold saline, chains of ganglia were dissected consisting of the head brain (HB) to at least midbody ganglion 8 (HB-G8) for recording the strength of the IPSCs and EPSCs in the central pattern generator interneurons.

The preparations were pinned (ventral surface up) in 60 mm Petri dishes lined with Sylgard™ (Dow Corning, Midland, MI). Ganglia in which heart interneurons were to be recorded were desheathed using fine scissors or microscalpels. The preparation was superfused continuously with normal leech saline containing (in mM): 115 NaCl, 4 KCl, 1.8 CaCl₂, 10 glucose, 10 HEPES buffer, adjusted to pH 7.4 with NaOH, at 1-2 ml/min (bath volume 6-8 ml). Heart interneurons were identified based on soma size, soma

location in the ganglion, and ultimately identified by their characteristic bursting activity. To provide uniformity in preparations every effort was made to keep dissections <1 hour and to minimize the number of ganglia desheathed. A total of 171 animals were used in this study.

Extracellular and intracellular recording techniques

We used conventional electrophysiological procedures for leech neurons described in Norris et al. (2007). For extracellular recordings from presynaptic heart interneurons, we used suction electrodes filled with normal saline. Electrodes were pulled on a Flaming/Brown micropipette puller (P-97, Sutter Instruments, Novato, CA) from borosilicate glass (1 mm o.d., 0.75 mm i.d., A.M. Systems) and placed in a suction electrode holder (E series, Warner Instruments Corp., Hamden, CT). To ensure a tight fit between the cell and electrode, the electrode tips had a final inner diameter of $\sim 20 \mu\text{m}$, approximately the diameter of a heart interneuron's soma. The electrode tip was brought in contact with the cell body and light suction was applied using a syringe until the entire cell body was inside the electrode. Extracellular signals were monitored with a differential A.C. amplifier (model 1700, A-M Systems, Carlsborg, WA) at a gain of 1,000 with the low and high frequency cut-off set at 100 and 1,000 Hz, respectively. Noise was reduced with a 60 Hz notch filter and a second amplifier (model 410, Brownlee Precision, Santa Clara, CA) amplified the signal appropriately for digitization. The HN(5) switch interneurons are very difficult to identify and record extracellularly because their somatic spikes are very small ($\sim 5 \text{ mV}$). To aid our search, we always monitored an easily identified and recorded front premotor interneuron. Signal to noise

ratios were often poor for the switch interneuron recordings, necessitating offline filtering so that the spikes could be easily discerned and detected.

For intracellular voltage and voltage-clamp recordings from postsynaptic heart interneurons, we used sharp intracellular electrodes (~20-30 M Ω filled with 4 M KAc, 20 mM KCl) and an Axoclamp-2B amplifier (Axon Instruments, Union City, CA) operating in discontinuous current-clamp or discontinuous single electrode voltage-clamp mode with a sample rate of 2.5 – 2.8 kHz. The electrode potential was monitored to ensure that it settled during each sample cycle. Output bandwidth was 0.3 kHz. Voltage-clamp gain was set at a minimum of 8nA/mV. The voltage-clamp holding potential for recording spontaneous IPSCs in interneurons was -45 mV and for recording spontaneous spike-mediated coupling currents was -55 mV. The minimum input resistance threshold required to voltage clamp any heart interneuron was set at 60M Ω (a value previously used in this system to ensure accurate measurements (Norris, Wenning et al. 2011)). At the end of each experiment the electrode was withdrawn from the neuron and only data in which the electrode potential was within ± 5 mV of ground were included. Thus all holding potentials were accurate within ± 5 mV.

Data were digitized (5 kHz sampling rate) using a digitizing board (Digi-Data 1200 Series Interface, Axon Instruments, Foster City, CA) and acquired using pCLAMP software (Molecular Devices, Sunnyvale CA) on a personal computer (Gateway Inc., Irvine CA).

Offline Data Analysis

Spike detection and IPSC/spike-mediated coupling current averaging were performed off-line using custom-made MATLAB software (Mathworks, Natick, MA); see Norris et al. (2006), and Norris et al. (2007) for more details. Each spike triggered average used at least 10 spike bursts and ignored the first 5 spikes in a burst (except when the presynaptic cell was HN(1) or HN(2) when no spikes were ignored due to the small number of average spikes per burst). The average strength of a synaptic connection was defined as the amplitude (measured from the preceding baseline current) of the largest peak of the spike-triggered average IPSC or spike-mediated coupling current.

In a number of cases (n=35) where the presynaptic cell was not recorded and the correct postsynaptic currents were clear and identifiable, hand measuring of the postsynaptic current was conducted. Hand measuring was done using Clampfit 9.0 Software (Molecular Devices, Sunnyvale CA) where the difference between the baseline and peak value were measured and recorded for each postsynaptic current in a burst (minus the first 5) over 10 individual bursts. The average postsynaptic current amplitude was used as the measure of synaptic strength. At each synapse input resistance was correlated with synaptic strength and variability within the recording was measured to assess for experimental artifacts.

When we compare the two types of synaptic connections (chemical inhibitory synapses and excitatory electrical junctions) we compare currents measured at the specified holding potential (inhibitory chemical connections $V_{\text{Hold}}=-45\text{mV}$ and excitatory electrical junctions $V_{\text{Hold}}=-55\text{mv}$). We infer that this comparison reflects the relative efficacy of the connection, but on an unknown absolute scale.

Statistics

Means are presented \pm standard deviation (s. d.) and in some cases the coefficient of variation (CV) was calculated. Current measurements were subjected to single factor ANOVA to determine significant differences between connections. F statistic, df , and p are reported. Where appropriate, post-hoc testing was done with Tukey's HSD test. In cases where ANOVA was not appropriate, we performed paired t -tests (two-tailed). For all tests $p < 0.05$ was the criterion for significant difference.

Results

Our present aim was to characterize as quantitatively as possible the strength of each synapse within the leech heartbeat central pattern generator and to examine the animal-to-animal variability and stereotypy that can underlie a circuit whose output is functionally stable. For the purposes of this analysis the circuit was broken up into functional sub-circuits: the timing network, the switch circuit, and the patterning circuit.

Timing Network: determining the strength of the coordinating heart interneuron IPSCs in the oscillator interneurons

To determine the strength of each inhibitory synaptic connection from a coordinating interneuron to a postsynaptic oscillator interneuron, we recorded extracellularly from one of the coordinating interneurons. We then voltage-clamped as many of the postsynaptic oscillator interneurons as possible in that preparation, recording spontaneous IPSCs for a minimum of 10 burst cycles in $n = 30$ total preparations.

Figure 2 illustrates a typical voltage clamp recording of the HN(3) oscillator interneuron (Fig. 2.A1) and the HN(4) oscillator interneuron (Fig. 2.A2) and extracellular recordings of the HN(2) and HN(1) coordinating heart interneurons, respectively. These oscillator interneurons receive predominantly spike-mediated synaptic transmissions from the coordinating interneurons and graded synaptic transmission is minimal (Olsen and Calabrese 1996);(Tobin and Calabrese 2005). Here we focused on the spike-mediated interactions using spike-triggered averaging of the spontaneous IPSCs.

The variability in the strength of these synapses is high, with each synapse varying approximately five-fold among individuals (Fig. 2B). For the HN(1) to HN(3) synapse $n=6$, $CV=0.45$, Average= $58.6\text{pA} \pm 26.2\text{pA}$. For the HN(1) to HN(4) synapse $n=6$, $CV=0.56$, Average= $73.8\text{pA} \pm 41.3\text{pA}$. For the HN(2) to HN(3) synapse $n=7$, $CV=0.55$, Average= $126\text{pA} \pm 69\text{pA}$. For the HN(2) to HN(4) synapse $n=16$, $CV=0.46$. Average= $80.9\text{pA} \pm 37\text{pA}$. Input resistance was not correlated with synaptic strength at any of these synapses. The average connection from the HN(2) coordinating interneuron to the HN(3) oscillator interneuron is stronger than the connection from the HN(2) coordinating interneuron to the HN(4) oscillator interneuron, $p=0.05$ (two-tailed, unpaired T-test.)

To explore the balance of inhibitory connections onto a single individual oscillator interneuron, we made simultaneous recordings from a single postsynaptic target (the HN(3) and HN(4) oscillator interneurons) and multiple presynaptic partners (the HN(2) coordinating interneuron and the contralateral HN(3) or HN(4) oscillator interneuron). In Figure 3 we illustrate this balance. In $n=5$ individuals we compared the strength of both inhibitory inputs onto the HN(3) oscillator interneuron. Measurements

made from the same individual are connected with a solid line. We can see that the balance of these two inputs is maintained with the inhibition from the coordinating interneuron being stronger than the inhibition from the contralateral oscillator interneuron ($R^2=0.93$, $p<0.01$). In $n=9$ individuals we compared the strength of both inhibitory inputs onto the HN(4) oscillator interneuron. Once again, individuals are connected with a solid line. In this comparison the balance between the two synaptic strengths was also very well maintained, with the inhibition from the contralateral oscillator interneuron being quite a bit stronger than the inhibition from the HN(2) coordinating interneuron ($R^2=0.52$, $p<0.005$). The maintenance of synaptic strength ratios is clearly important at these synapses.

The Timing Network: Determining the strength of the HN(3) and HN(4) interneuron-mediated IPSCs and the HN(3) interneuron-spike-mediated coupling currents in the HN(3) and HN(4) oscillator interneurons.

To determine the strength of the HN(3) and HN(4) interneuron-mediated IPSCs in their contralateral partner, we recorded extracellularly from one of the oscillator interneurons. We then voltage-clamped the postsynaptic partner in that preparation, recording spontaneous IPSCs for a minimum of 10 interneuron burst cycles in a total of $n = 30$ preparations.

Figure 4A illustrates a typical voltage-clamp recording of the postsynaptic HN(3) oscillator interneuron and an extracellular recording of the presynaptic, contralateral HN(3) oscillator interneuron. Graphs in Figure 4C illustrate the tremendous variability seen in the strength of the reciprocal inhibitory synapses between these two half-center

oscillators. For the HN(3) to HN(3) synapse $n=10$, $CV=0.43$, average= $97.3\text{pA} \pm 41.6\text{pA}$. For the HN(4) to HN(4) synapse $n=23$, $CV=0.67$, average= $161.1\text{pA} \pm 107.3\text{pA}$. Input resistance was not correlated with synaptic strength at either of these synapses. There was no difference in the strength of the average synapse between the HN(3) oscillator interneurons and the average synapse between the HN(4) oscillator interneurons, $p>0.05$ (two-tailed, un-paired T-Test).

To determine the strength of the electrical connection from the HN(3) oscillator interneuron to the HN(4) oscillator interneuron, we recorded extracellularly from the HN(3) oscillator interneuron ($n = 7$) and then voltage clamped the ipsilateral HN(4) oscillator interneuron (Fig. 4B). The graphs in Figure 4C illustrate the nearly 5-fold range in synaptic strength seen between individuals in this electrical connection with $CV=0.70$ and average= $90\text{pA} \pm 63\text{pA}$. Input resistance was not correlated with synaptic strength at this synapse.

The HN(4) oscillator interneurons allows us another interesting comparison point, within one individual, for looking at the balance of multiple synapses onto a single postsynaptic target. The HN(4) oscillator interneuron receives an electrical connection from the ipsilateral HN(3) oscillator interneuron as well as an inhibitory input from the contralateral HN(4) half-center partner interneuron. In Figure 5 a comparison was made in $n=5$ individuals that shows no clear-cut trend between these two connections in a single postsynaptic target. In three individuals, the synaptic strengths were nearly equivalent, with the electrical connection slightly stronger than the inhibitory synapse. In one individual the electrical connection was nearly 8 times stronger than the inhibitory

connection, and in the final individual the inhibitory connection was nearly twice as strong as the electrical connection.

The Switch Network: Determining the strength of the HN(3) and HN(4) oscillator interneuron mediated inhibitory inputs onto the HN(5) switch interneuron

To assess the strength and variability of this part of the circuit we recorded extracellularly from the presynaptic oscillator interneurons in ganglia 3 (n=6), 4 (n=7), or 3 and 4 (n=2) and voltage clamped the postsynaptic switch interneuron recording the IPSCs elicited by spikes in the oscillator interneuron (Fig. 6A). Figure 6B illustrates the nearly six-fold range in variability for the HN(3) to HN(5) synapse n=8, CV=0.89, and average=65.3pA +/- 58.2pA. For the HN(4) to HN(5) synapse n=9, CV=0.64 and average=67.8pA +/- 43.5pA. Input resistance was not correlated with synaptic strength at either of these synapses. No difference was seen in the synaptic strength of the HN(3) and HN(4) oscillator interneuron inputs onto the HN(5) switch interneurons when the switch interneuron was in the active vs. inactive state. Nor was any difference in synaptic strength found between the HN(3) to HN(5) and HN(4) to HN(5) synapses.

The Patterning Circuit: Determining the strength of the HN(5) interneuron-mediated IPSCs and the HN(3) and HN(4)-interneuron spike-mediated coupling currents in the HN(6) and HN(7) middle premotor interneurons.

Each middle premotor interneuron receives excitatory input from the ipsilateral oscillator interneurons through electrical junctions and synaptic inhibition from both switch interneurons (each HN(5) switch interneuron makes bilateral inhibitory synapses),

although only one is rhythmically active at a time. To determine the strength of each inhibitory synaptic connection from a switch interneuron to a middle premotor interneuron (Fig. 7), we recorded extracellularly from one (a minority of cases, $n = 8$) or both ($n = 17$) switch interneurons. When we recorded only one HN(5) switch interneuron we inferred the synaptic strength of its contralateral homolog in the same middle premotor interneuron, during the recorded switch interneuron's silent state, by manually measuring and averaging the spontaneous rhythmic IPSCs phase-locked with the activity of the monitored oscillator interneuron IPSCs. When both HN(5) switch interneurons were recorded, direct comparisons of spike-triggered averaged IPSCs were made.

Figure 7B illustrates the tremendous variability seen in inhibitory synaptic strength from the switch interneurons onto the middle premotor interneurons (both ipsilateral (i) and contralateral (c).) For the HN(5) to HN(6i) synapse $n=9$, $CV=0.47$, and average= $70.3\text{pA} \pm 33.4\text{pA}$. For the HN(5) to HN(6c) synapse $n=7$, $CV=0.57$, and average= $35.9\text{pA} \pm 20.6\text{pA}$. For the HN(5) to HN(7i) synapse $n=14$, $CV=0.50$, and average= $155.6\text{pA} \pm 78.5\text{pA}$. For the HN(5) to HN(7c) synapse $n=13$, $CV=0.37$, and average= $75.3\text{pA} \pm 27.8\text{pA}$. Input resistance was not correlated with synaptic strength at any of these synapses.

On average, in both middle premotor interneurons the ipsilateral HN(5) switch interneuron synapse was stronger than the corresponding contralateral synapse (in ganglion 6 $p<0.05$ and in ganglion 7 $p<0.05$ with a two-tailed, un-paired T-Test.) On average, the ipsilateral synapses onto the HN(6) middle premotor interneuron were weaker than the ipsilateral synapses onto the HN(7) middle premotor interneuron ($p<0.05$ with a two-tailed, unpaired T-test.) These average comparisons were explored further by

direct comparisons within individuals to confirm these average differences (Fig. 8).

When we compared within $n=4$ individuals, we observed that the ipsilateral synapse was not universally larger than the contralateral synapse.

To determine the strength of each electrical connection from an oscillator interneuron to a middle premotor interneuron (Fig. 9), we recorded extracellularly from one ($n = 23$) or both ($n = 12$) oscillator interneurons. We then voltage clamped the ipsilateral middle premotor interneurons, recording spike-mediated coupling currents for a minimum of 11 interneuron burst cycles. To assess the impact of switches in coordination mode on the spike-mediated coupling currents, continuous voltage clamp measurements were made across a minimum of 2 switches. Synchronous and peristaltic coordination modes were compared with a paired, 2-tailed t -test.

Within a single individual, the strengths of these four electrical connections all fell within the same range, however the actual strength varied among synapses (Fig. 9B). These electrical connections varied in strength over a three to five fold range between individuals (Fig. 9C). For the HN(3) to HN(6) synapse $n=15$, $CV=0.39$ and average= $84.4\text{pA} \pm 33.1\text{pA}$. For the HN(4) to HN(6) synapse $n=16$, $CV=0.41$ and average= $78.3\text{pA} \pm 32.3\text{pA}$. For the HN(3) to HN(7) synapse $n=18$, $CV=0.29$ and average= $70.7\text{pA} \pm 20.6\text{pA}$. For the HN(4) to HN(7) synapse $n=13$, $CV=0.52$ and average= $72\text{pA} \pm 37.5\text{pA}$. Input resistance was not correlated to synaptic strength at any of these synapses.

A similar comparison as before was made with multiple presynaptic partners onto the same postsynaptic target within individuals. In this case (Fig. 10), we compared the input of the HN(3) and HN(4) oscillator interneurons both onto either the HN(6) or the

HN(7) middle premotor interneuron. We compared these electrical junctions in n=6 individuals and observed that although there is a trend for the connection from the HN(4) oscillator interneuron to be stronger than that from the HN(3) oscillator interneuron, there is no strict relationship. In general, all of these electrical connections were within a similar range in a single individual.

The balance between excitatory and inhibitory input was examined in preparations where the presynaptic input of both an oscillator interneuron and the switch interneuron could be simultaneously recorded during the voltage clamp recording of a middle premotor interneuron. Figure 11 illustrates the inputs for the HN(3) to HN(6) synapse and HN(5) to HN(6i) synapse (n=6), where there was no correlation between the inhibitory synaptic inputs from the switch interneuron and the excitatory coupling currents from the middle premotor interneurons. For the HN(3) to HN(7) synapse and the HN(5) to HN(7i) synapse (n=5), we did observe a correlation that indicates that the maintenance of synaptic strength ratios is important at these synapse ($R^2=0.58$, $p<0.05$).

Discussion:

Inputs from the coordinating interneurons vary 5-fold between individuals

The strength of the inhibitory connections from the coordinating interneurons in ganglia 1 and 2 onto the oscillator interneurons in ganglia 3 and 4 varied 5-fold between individuals (Fig 2B.) This high degree of variability indicates that the network has the ability to maintain its stereotyped output over a range of synaptic strengths. Since the inputs from the coordinating interneurons onto the oscillator interneurons shape the rhythm but do not appear to play a critical role in establishing proper phasing (Jezzini,

Hill et al. 2004), it is not surprising that this synapse would exhibit a large variability in synaptic strength.

When examining this connection it was also important to look at the comparison of the strength of the two inputs to each of the oscillator interneurons (inhibition from the coordinating interneurons as well as inhibition from the contralateral half center partner.) Based on predictions generated by our model of the timing network of the leech heartbeat CPG, we hypothesized that the inhibitory input from the contralateral half center partner interneuron would be stronger than the inhibitory input from the ipsilateral coordinating interneuron (Jezzini, Hill et al. 2004).

When comparing the balance of inhibition onto the HN(3) oscillator interneuron from the ipsilateral HN(2) coordinating interneuron and the contralateral HN(3) oscillator interneuron we found that a strict balance of relative strengths did not exist within a single individual (Fig 3C1) In general, the strengths of the two inputs were very similar in a single individual with the inhibition from the coordinating interneuron generally being slightly stronger than the inhibition from the oscillator interneuron. Interestingly, in our comparison of the inhibition onto the HN(4) oscillator interneuron from the ipsilateral HN(2) coordinating interneuron and the contralateral HN(4) oscillator interneuron (Fig 3C2), we found an example of where the ratio of synaptic strengths is maintained, with the inhibitory input from the contralateral oscillator interneuron being much stronger than the inhibitory input from the ipsilateral coordinating interneuron.

The weaker input from the coordinating interneurons onto the oscillator interneurons in ganglion 4 would allow for an earlier return from inhibition in the HN(4) interneurons, causing a shorter period in that ganglion. The HN(4) half-center oscillator

pair typically leads the HN(3) half-center oscillator pair in phase, and this finding could help to explain how this phase difference was generated. In the occasional case where the input from the coordinating interneuron was weaker than the input from the contralateral HN(3) oscillator interneuron, it would make sense that the HN(3) oscillator pair would then lead the HN(4) oscillator pair, a case that is seen occasionally in the biology (Masino and Calabrese 2002) .

In the case of the inhibitory connections onto the oscillator interneurons in ganglion 4 we see a clear case of where the ratios of synaptic strength between the two synapses is maintained in the individuals (Fig. 3C2). In contrast to the idea that the total synaptic weight onto a target is the important end result, we see that the strength of the two inhibitory synapses is strongly correlated with a stronger HN(2) coordinating interneuron synapse occurring in the same individual as a stronger HN(4) oscillator interneuron synapse.

Synapses within the half-center oscillators vary up to 14-fold between individuals

It is the reciprocal inhibitory connections between members of each half-center oscillator that are critical in establishing the bursting behavior of the rest of the circuit and setting up the functional basis for the side-to-side alternation of the heartbeat. It seems reasonable to suppose that these critically important synapses would have a small amount of variability due to their vital role in establishing heartbeat.

Clearly, despite the importance of the half center in setting up the side to side oscillations in the network it is able to accommodate quite a bit of variability in synaptic strength (5-fold in HN(3) to HN(3) synapse and 14-fold in the HN(4) to HN(4) synapse)

(Fig. 4C.) No significant difference exists between the strength of the HN(3) to HN(3) synapse and the strength of the HN(4) to HN(4) synapse, so it would seem that as long as these two oscillator cells are coupled via reciprocal inhibition at some strength they are able to set up the essential oscillations that the network relies on.

The two half center oscillators are electrically coupled via a strong connection from the HN(3) to the HN(4) interneuron in ganglion 4 (Thompson and Stent 1976c), although systematic measurements had not been done before this study. We hypothesized that this connection serves to couple the two oscillators, allowing them to oscillate nearly in phase (ipsilateral HN(3) to HN(4) oscillator interneurons). This connection varies nearly 12-fold between individuals (Fig. 4C).

This electrical connection allows two pairs of reciprocally inhibitory oscillator interneurons to synchronize. When making a comparison of the input from the electrically connected HN(3) oscillator interneuron onto the HN(4) oscillator interneuron with the inhibition from the contralateral HN(4) oscillator interneuron (Fig. 5) we see that no clear relationship between these two inputs emerges. In a few individuals, we see that the synaptic strengths of the electrical connection and inhibitory input are very similar. In other individuals the electrical connection is substantially stronger (30-100pA) than the inhibitory input, while in still other individuals the inhibitory input is stronger (~40pA) than the electrical connection.

This unpredictable pattern may be due to the fact that we are not getting the full picture of the inputs onto the HN(4) interneuron in this comparison. In our other comparisons we are looking at the full complement of presynaptic inputs onto a single postsynaptic target, while in this instance we are not considering the inputs from the

coordinating interneurons in ganglia 1 and 2. The total input onto the HN(4) oscillator interneurons may be the important factor in balancing these synaptic strengths, as it appears there is no maintenance of synaptic strength ratio between these two important synapses.

Synapses onto the HN(5) switch interneuron vary 10-fold between individuals

The oscillator interneurons synapse onto the HN(5) switch interneuron with inhibitory connections (Fig. 6A). The switch interneurons are extremely important to the circuit, because they are causing the critical switch in coordination mode of the heart tubes by shifting the phasing of the middle and rear premotor interneurons with respect to the timing network. The relative phase relationships of the premotor interneurons are important in providing coordination mode information to the heart motor neurons. The inhibitory inputs onto the HN(5) switch interneurons from the oscillator interneurons are extremely important to the eventual motor output of the network because they are the only way for the switch interneurons to be coordinated with the bursting of the timing network and to therefore provide their inhibition at the appropriate time onto the middle premotor interneurons.

The inhibitory synaptic inputs from the oscillator interneurons that help to shape the bursting behavior of the switch interneurons (and therefore the rest of the CPG) vary nearly 10-fold between individuals (Fig. 6B). Once again, it would seem that as long as the information is passed from one interneuron to the next, the absolute strength of the connection is not critical in generating network output. The HN(5) interneurons receive input only from the oscillator interneurons, and so there is no balance of electrical

connection and inhibitory connection to take into account. In a small number of individuals (n=3), the HN(3) and the HN(4) oscillator interneurons were simultaneously recorded while voltage clamping the HN(5) switch interneuron, and in each case the inhibition from the HN(4) interneuron was slightly stronger than the inhibition from the HN(3) interneuron (data not shown.)

Inputs onto the middle premotor interneurons vary 3 to 12-fold between individuals

The middle premotor interneurons receive inhibition from both the ipsilateral HN(5) switch interneuron and the contralateral HN(5) switch interneuron as well as an electrical connection from both the HN(3) and HN(4) oscillator interneurons. The balance between these opposing inputs must provide appropriate phasing information. Therefore, the connections onto these middle premotor interneurons and the balance between them are critically important in generating the appropriate phasing of each coordination mode.

On the synchronous side (where the switch interneuron is rhythmically active), the excitation due to ipsilateral oscillator interneuron input arrives roughly in anti-phase with the inhibitory input from the switch interneurons, whereas on the peristaltic side (switch interneuron silent) this excitatory electrical input arrives roughly in phase with the inhibitory inputs from the contralateral switch interneuron (Fig. 7A). The observed outcome of these inputs is that each of the four middle premotor heart interneurons fires at a different phase. The complex nature of the connections onto the middle premotor interneurons and the phasing of these interneurons suggests that the proper phasing of the middle premotor interneurons results from a balance of excitatory drive (from electrical

coupling) and inhibition, and that for each of the four middle premotor interneurons, this balance will be slightly different.

While constructing an accurate model of the complete heartbeat CPG, it became quickly obvious that a specific balance must exist between electrical excitation and chemical inhibition for each middle premotor interneuron to allow the network to produce its stereotyped phasing and output in these four different middle premotor interneurons (Weaver, Roffman et al. 2010). How do these four middle premotor heart interneurons fire in different phases both ipsilaterally and contralaterally? Do the connections differ among them (either side-to-side and/or onto the different ganglia) in strength or dynamics?

Our complete CPG model more importantly predicts that each of the four synapses from the switch interneuron onto the middle premotor heart interneurons will exist at a different relative strength (Weaver, Roffman et al. 2010). In order to mimic the proper output of the circuit, the complete CPG model had to be tuned such that the HN(5) inhibitory synapses onto the ipsilateral middle premotor interneuron were stronger than the synapses onto the contralateral middle premotor interneuron. The complete CPG model also required that these synapses onto the interneurons in ganglion 7 be stronger than similar synapses onto the interneurons in ganglion 6 (Weaver, Roffman et al. 2010).

Both of these predictions were shown to be correct with this set of experiments. First, the complete CPG model predicted that the synapses from the ipsilateral HN(5) switch interneurons would be stronger than the synapses from the contralateral HN(5) switch interneurons. This was found to be true on average ($P < 0.05$ in a two-tailed, unpaired T-Test) despite high levels of variability between individuals (Fig 7B).

The comparison between the ipsilateral and contralateral HN(5) switch interneuron inputs onto a single postsynaptic target in both the HN(6) and HN(7) middle premotor interneuron can be made in individuals as well (Fig 8). In three of the four individuals in which this comparison was made, we see a large difference in the inhibitory synaptic strength between the ipsilateral and contralateral connections, with the ipsilateral connection being the stronger. For both the HN(6) and HN(7) middle premotor interneurons there is a single individual where this relationship does not hold, however this is likely not due to injury in the individual, as this anomaly occurs in different individuals for the two comparisons.

The complete CPG model also predicted that the inhibitory inputs onto the HN(7) interneuron will be stronger than the inputs onto the HN(6) interneurons. This comparison can only be made using averages across experiments (since we are dealing with two different postsynaptic targets). We see that both the ipsilateral and contralateral connections are stronger in the HN(7) middle premotor interneuron than they are in the HN(6) middle premotor interneuron ($P < 0.05$ for the ipsilateral connections using a two-tailed, unpaired T-Test and $P < 0.005$ for the contralateral connections using a two-tailed, unpaired T-Test) (Fig 7B).

In building the complete CPG model two simplifying assumptions were made that were tested here (Weaver, Roffman et al. 2010). 1) Electrical coupling from a given ipsilateral oscillator interneuron onto a given middle premotor interneuron is identical on each side i.e. there is neither a systematic left-right asymmetry in the nerve cord nor any mechanism to alter coupling with changes in coordination mode. 2) Electrical coupling from each ipsilateral oscillator interneuron is the same onto both pairs of middle

premotor interneurons (This later assumption is not necessary, but simplified the analysis).

On average, the electrical connections onto the middle premotor interneurons in ganglia 6 and 7 are the same strength (Fig. 9C). We see no significant difference from side-to-side nor between ganglia in the strength of these electrical connections. When we compare within a single individual (Fig. 9B), we can see that these connections, although slightly different, are all very close in strength, confirming that the simplifying assumptions used in the building of the complete CPG model were valid.

When comparing across several individuals (Fig. 10) a general trend does emerge in which the electrical connection from the HN(4) oscillator interneuron is stronger than the electrical connection from the HN(3) oscillator interneuron, although there are a few individuals in which this generalization does not hold true. It would be interesting to note if these instances in which the HN(3) oscillator interneuron electrical connection is stronger are the same individuals in which the HN(3) oscillator pair leads the HN(4) oscillator pair in phase (and in which the connection from the HN(2) coordinating interneuron onto the HN(3) oscillator interneuron is stronger than the inhibitory connection from the contralateral HN(3) oscillator interneuron), however this comparison was never made.

The relative balance of excitatory electrical coupling from the oscillator interneurons and inhibitory inputs from the switch interneuron is extremely important in establishing the synchronous and peristaltic phasing for the motor output of the CPG from ganglia 3 through ganglia 18. From the perspective of a single pair of middle premotor

interneurons, their different phases (side-to-side) can only be accounted for by different relative timing of their inhibitory synaptic input with respect to electrical coupling currents and the difference in strength of their connections. Thus, each interneuron in a premotor interneuron pair serves as a valuable counterpoint for the other in understanding the functional implications of the synaptic inhibition and electrical coupling interaction.

We are able to make a few comparisons of this electrical/inhibitory balance in individuals to explore how each individual solves this important problem (Fig 11). When comparing the inhibitory input from the HN(5) switch interneuron onto the ipsilateral HN(6) middle premotor interneuron with the electrical connection from the HN(3) oscillator interneuron onto the HN(6) middle premotor interneuron, we see no clear pattern emerge. In several individuals the electrical connection is larger than the inhibitory connection, while in others the inhibitory connection is larger. When comparing those same inputs onto the HN(7) middle premotor interneuron, however, there is a very stereotyped balance with the inhibitory input from the ipsilateral HN(5) switch interneuron larger than the electrical connection from the HN(3) oscillator interneuron.

Is all of this variability simply experimental artifact?

Previous work in both the leech heartbeat system (Norris, Weaver et al. 2006) (Norris, Wenning et al. 2011) and the stomatogastric nervous system of the lobster (a central pattern generating circuit that is responsible for the rhythmic chewing and filtering behavior in the lobster foregut) (Marder and Goaillard 2006; Schulz, Goaillard et al. 2007) has suggested a 2 to 4 fold animal to animal variability in both intrinsic

properties and synaptic strengths despite a relatively stable circuit output. Our studies confirm this wide variability, with observed variations of 3 to 16 fold between individuals for the strength of synapses within the leech heartbeat central pattern generator.

The simplest explanation for this tremendous variability between individuals is simple experimental artifact. Numerous precautions were taken to avoid this and several post-hoc measurements were taken to assure that this was not the case. During our experiments we adhered to a strict minimum input resistance in the voltage clamped postsynaptic cell to guarantee a healthy cell and valid penetration. This minimum input resistance has been used successfully before (Norris, Wenning et al. 2011) in this system to ensure accurate measurements. During analysis the within animal variability was assessed for each synapse and was found to be insignificant in every case over the duration of the recording. In analyzing our data, we looked for a correlation between input resistance and synaptic strength at each synapse and never found any significant correlation between the two. Lastly, the correlations between inhibitory and electrical connections in key post-synaptic targets (the correlation between the HN(2) to HN(4) synapses and the HN(4) to HN(4) synapse as well as the correlation between then HN(5) to HN(6i) synapse and the HN(3) to HN(6) synapse) indicate that this is true animal to animal variability rather than measurement error.

Heartbeat is a critically important and requisite activity for life, and the leeches used in these experiments have lived at least a full year before being used for these experiments. This indicates that the resultant heartbeat from each of the measured circuits was sufficient to allow the animal to live a normal life and to grow from hatchlings, through the juvenile stage, into mature adults. Thus, each of the leech

heartbeat central pattern generator networks that we used for our experiment can be considered representative of the natural population. It would follow, then, that the variability that we have reported can be considered an accurate representation of the variability that exists within the natural population. Natural differences in genetics and experience could influence the circuit and lead to differences in synaptic strength and potentially a variety of other cellular and network characteristics.

Modeling work in the stomatogastric ganglion has indicated that it may not necessarily be synapse strengths but maybe synaptic ratios that are important in circuit function (Hudson and Prinz 2010). The importance of synaptic ratios agrees with what we have seen in this study, where there is tremendous variability in the actual synaptic strengths between individuals, but there do appear to be several points (that we can measure and accurately compare) where the ratio of the two synapses appears to be maintained (for example, the HN(2) to HN(4) synapse compared to the HN(4) to HN(4) synapse or the HN(5) to HN(7i) synapse compared to the HN(3) to HN(7) synapse.)

The maintenance of relative synaptic strengths throughout the network to maintain global firing properties (outputs) is present in this network. Such maintenance has the right characteristics to preserve relative differences in synaptic strengths that are necessary for phase maintenance, while allowing a neuron to adjust the total amount of synaptic excitation or inhibition that it receives. The maintenance of relative synaptic strength between network components that we see here indicates that several synaptic relationships measured in this study are critical for the maintenance of network output.

In contrast to the idea of a maintenance in the ratio of synaptic strengths, recent computational work by Taylor et al (2009) indicates that a strong correlation between

cellular parameters may not be necessary for cells to give rise to functionally similar outputs. Despite the fact that we see significant correlations between several synapse pairs, it is a possibility that these correlations are not a necessity for the correct circuit output but rather a consequence of activity dependent regulation over time. The compensatory methods that presumably played a role in the tremendous synaptic variability may have simply co-varied certain synaptic strengths. This would create the perception of important “balances” when in fact these balances are not necessary for the correct circuit output and network dynamics at all.

How exact do synapse strengths really need to be?

In 2001, Edelman and Galley showed in a single cell organism that it is not necessary to specify the exact number of ion channels or receptors that each neuron should express, either during development or over the lifetime of the neuron and animal (Edelman and Galley 2001). Using a single cell organism showing variability in mRNA and proteins, they showed that ongoing activity-dependent rules of various kinds can be used to modify receptor and channel numbers and distributions to maintain target circuit performance despite ongoing channel and receptor turnover. This idea of biological degeneracy supports our findings here that a specific set synaptic strengths is not the important factor in a central pattern generating network.

In fact, Padmanabhan and Urban (2010) suggest that variability in network components and neuronal function may prove to be computationally advantageous for the system. The variability in intrinsic functions of neurons (and by extension, synaptic strengths) allows for neurons to code for far more information than homogeneity would

allow. The idea that an increase in variability would allow for greater computational power indicates that variability is biologically advantageous and may not simply be the result of some biological imprecision.

Where do you go from here?

One of the large, unanswered questions that this study raises is how can the circuit tolerate so much variability? Two logical answers for this question are that the synapse itself isn't critical for correct network output (although we know that this cannot be the case for some of the synapses in the leech heartbeat CPG) or there are compensatory changes elsewhere in the circuit that we did not identify with this set of experiments. In this study we focused on synaptic strengths, largely ignoring intrinsic properties (except for input resistance). Any changes in intrinsic properties of the leech heartbeat interneurons that would serve to balance out this tremendous variability in synaptic strength would have gone undetected. Additionally, there are many different combinations of synapses within the CPG that we have not correlated within a single individual. Due to the potential damage to a neuronal cell body caused by intracellular recording and voltage clamp measurements we are unwilling to correlate the synaptic strength of two synapses that do not share an identical postsynaptic target (and therefore a single voltage clamp experiment).

The ideal experiment, then, measures as many aspects of the circuit as possible in a single preparation. This approach, championed by Goillard et al. (2009) would require the acquisition of as much data as possible from a single preparation including information about both intrinsic properties and synaptic strengths. This ideal experiment

is extremely difficult in a system such as the leech heartbeat, where we are only able to keep our preparations alive for a few hours in vitro. This type of experiment is better suited for a system such as the stomatogastric ganglion, where an individual preparation can be kept alive for many hours and even days in vitro.

An interesting follow-up to this study would include an in-depth look at one aspect of the circuit with correlations of all synaptic strengths and intrinsic properties with the functional outputs of the circuit and the heartbeat system in general. The timing circuit is ideal for this comparison based on the small number of neurons and connections (4 bilateral pairs of neurons with 7 connections) as well as some interesting correlations between inputs that have arisen from this study (most notably the correlations of the coordinating interneuron HN(2) input onto the oscillator interneurons and the input from the contralateral oscillator interneuron in both ganglia 3 and 4.) This set of heart interneurons is also relatively easy to locate and record from and this set of experiments would require less dissection and fewer ganglia to be desheathed both minimizing the risk for injury and reducing time spent preparing the nerve cord for the experiment.

Lastly, a look into how this variability arises developmentally would be very interesting in this network. Is this wide range of naturally occurring synaptic strengths present from birth or is the range acquired over a lifetime of activity dependent regulation and experience?

Figure Legends:

Figure One:

Circuit diagram illustrating synaptic connections among heart interneurons (HN) and the coordination modes associated with a switch in activity state of the switch interneurons. Lines indicate cell processes, small colored/black circles indicate inhibitory synaptic chemical connections and diodes indicate electrical connections. Cells with similar input and output connections and function are depicted as one. Color scheme is maintained throughout, e.g. red color denotes HN(1) and HN(2), the coordinating interneurons. In all figures, interneurons are indexed by body side and ganglion number.

Figure Two:

(A1): The coordinating interneurons in ganglia 1 and 2 have inhibitory chemical synaptic connections onto the oscillator interneurons in ganglia 3 and 4. An HN(L,3) oscillator interneuron was voltage clamped ($V_{\text{Hold}}=-45\text{mV}$) while simultaneously recording extracellularly from the HN(L,2) presynaptic coordinating interneuron. Symbols in the expanded recording indicate postsynaptic currents attributable to spiking activity in the HN(L,2). (A2): An HN(L,4) oscillator interneuron was voltage clamped ($V_{\text{Hold}}=-45\text{mV}$) while simultaneously recording from the HN(L,1) presynaptic coordinating interneuron. Symbols in the expanded recording indicate postsynaptic currents attributable to spiking activity in the HN(L,1). (B): Synaptic strength and animal to animal variability of the coordinating interneuron to oscillator interneuron synapse indicated in pA. Data is plotted with individual points (circles), quartiles (squares indicate median while solid lines indicate 25th/75th quartiles), and averages with standard deviation (diamonds). The

spike triggered averages shown are from the ends of the spectrum with each representative point indicated. For the HN(1) to HN(3) synapse $n=6$, $CV=0.45$, Average= $58.6\text{pA} \pm 26.2\text{pA}$. For the HN(1) to HN(4) synapse $n=6$, $CV=0.56$, Average= $73.8\text{pA} \pm 41.3\text{pA}$. For the HN(2) to HN(3) synapse $n=7$, $CV=0.55$, Average= $126\text{pA} \pm 69\text{pA}$. For the HN(2) to HN(4) synapse $n=16$, $CV=0.46$, Average= $80.9\text{pA} \pm 37\text{pA}$.

Figure Three:

(A1) An HN(L,3) oscillator interneuron was voltage clamped ($V_{\text{Hold}}=-45\text{mV}$) while simultaneously recording extracellularly from the ipsilateral HN(L,2) coordinating interneuron and the contralateral HN(R,3) oscillator interneuron, both presynaptic. (A2): An HN(L,4) oscillator interneuron is voltage clamped ($V_{\text{Hold}}=-45\text{mV}$) while simultaneously recording extracellularly from the ipsilateral HN(L,2) coordinating interneuron and the contralateral HN(R,4) oscillator interneuron both presynaptic (B1): Spike triggered averages from the HN(2) to HN(3) and HN(3) to HN(3) synapse within a single individual are overlaid to emphasize the strength difference. This strength difference is also seen in voltage recordings (not shown). (B2): Spike triggered averages for the HN(2) to HN(4) and HN(4) to HN(4) synapse within a single individual are overlaid to illustrate the large strength difference between these two synapses. This strength difference is also seen in voltage recordings (not shown). (C1 and C2): Corresponding synaptic strength measurements from the ipsilateral coordinating interneuron and the contralateral oscillator interneuron within a single animal are linked

with a single line to illustrate the maintenance of synaptic strength ratios that occurs within these synapses.

Figure Four:

(A): The postsynaptic HN(R,3) oscillator interneuron is voltage clamped ($V_{\text{Hold}}=-45\text{mV}$) with the presynaptic HN(L,3) oscillator interneuron recorded extracellularly. Spike triggered averaging is used to assess synaptic strength of the inhibitory connection. (B):

The postsynaptic HN(L,4) oscillator interneuron is voltage clamped ($V_{\text{Hold}}=-55\text{mV}$) with the presynaptic HN(L,3) oscillator interneuron recorded extracellularly. Spike triggered averaging is used to assess synaptic strength of the electrical connection. (C):

Synaptic strength and animal to animal variability within the half center oscillator synapses are shown in pA. Data is plotted with individual points (circles), quartiles (squares indicate median while solid lines indicate 25th/75th quartiles), and averages with standard deviation (diamonds). The spike triggered averages shown are from the ends of the spectrum with each representative point illustrated. For the HN(3) to HN(3) synapse $n=10$, $CV=0.43$, average= $97.3\text{pA} \pm 41.6\text{pA}$. For the HN(4) to HN(4) synapse $n=23$, $CV=0.67$, average= $161.1\text{pA} \pm 107.3\text{pA}$. For the HN(3) to HN(4) electrical connection $n=7$, $CV=0.70$ and average= $90\text{pA} \pm 63\text{pA}$.

Figure Five:

The oscillator interneurons in ganglion 4 receive both synaptic inhibition from their half center partner as well as excitatory coupling currents from the ipsilateral oscillator interneuron in ganglion 3. This balance of excitation and inhibition is a potential control

point for the system's variable synapses. A comparison was made within $n=5$ individuals with no significant correlation in synaptic strength. Each individual pair connected with a solid line is from a single individual.

Figure Six:

(A): The oscillator interneurons in ganglia 3 and 4 have an inhibitory chemical synapse onto the ipsilateral switch interneuron in ganglion 5. A postsynaptic, voltage clamp recording of the HN(L,5) switch interneuron ($V_{\text{Hold}}=-45\text{mV}$) and a presynaptic extracellular recording of both the HN(L,3) oscillator interneuron and the HN(L,4) oscillator interneuron are shown. (B): Synaptic strength and animal to animal variability of the inhibitory chemical connection from the half center oscillator interneurons onto the HN(5) switch interneuron are shown. Data is plotted with individual points (circles), quartiles (squares indicate median while solid lines indicate 25th/75th quartiles), and averages with standard deviation (diamonds). The representative spike triggered averages were chosen to illustrate the range of strengths observed. For the HN(3) to HN(5) synapse $n=8$, $\text{CV}=0.89$, and $\text{average}=65.3\text{pA} \pm 58.2\text{pA}$. For the HN(4) to HN(5) synapse $n=9$, $\text{CV}=0.64$ and $\text{average}=67.8\text{pA} \pm 43.5\text{pA}$.

Figure Seven:

(A): Simultaneous extracellular recordings of both HN(5) switch interneurons and a concurrent voltage clamp recording of the HN(7) middle premotor interneuron ($V_{\text{Hold}}=-45\text{mV}$). During the peristaltic coordination mode (the first half of the recording) the contralateral HN(5) switch interneuron is active and after the switch (the second half of

the recording) the ipsilateral HN(5) switch interneuron is active. Expanded traces and spike triggered averages illustrate the magnitude difference between an ipsilateral and contralateral connection within the single, example individual. (B): Synaptic strength and animal to animal variability of the inhibitory chemical connection from both HN(5) switch interneurons onto the middle premotor interneurons is shown. Data is plotted with individual points (circles), quartiles (squares indicate median while solid lines indicate 25th/75th quartiles), and averages with standard deviation (diamonds). Spike triggered averages are representative of the range of synaptic strengths observed. For the HN(5) to HN(6i) synapse $n=9$, $CV=0.47$, and average= $70.3\text{pA} \pm 33.4\text{pA}$. For the HN(5) to HN(6c) synapse $n=7$, $CV=0.57$, and average= $35.9\text{pA} \pm 20.6\text{pA}$. For the HN(5) to HN(7i) synapse $n=14$, $CV=0.50$, and average= $155.6\text{pA} \pm 78.5\text{pA}$. For the HN(5) to HN(7c) synapse $n=13$, $CV=0.37$, and average= $75.3\text{pA} \pm 27.8\text{pA}$.

Figure Eight:

The middle premotor interneurons in ganglia 6 and 7 receive synaptic inhibition from both the ipsilateral and contralateral HN5 switch interneuron. A comparison of the strength of these synapses was made within $n=4$ individuals. Each individual is illustrated with a separate icon and each single postsynaptic voltage clamp recording is connected with a solid line.

Figure Nine:

(A1): Simultaneous extracellular recordings of both the HN(R,3) and the HN(R,4) oscillator interneurons and a voltage clamp recording of the HN(R,6) middle premotor

interneuron ($V_{\text{Hold}}=-55\text{mV}$) are shown to illustrate the electrical connection. (A2): Simultaneous extracellular recordings of both the HN(R,3) and the HN(R,4) oscillator interneurons and a voltage clamp recording of the HN(7) middle premotor interneuron ($V_{\text{Hold}}=-55\text{mV}$). (B): Sample spike triggered averages from a single individual are shown. (C): Synaptic strength and animal to animal variability of the electrical connection from both oscillator interneurons onto the middle premotor interneurons is shown. Data is plotted with individual points (circles), quartiles (squares indicate median while solid lines indicate 25th/75th quartiles), and averages with standard deviation (diamonds). Spike triggered averages are representative of the range of synaptic strengths observed. For the HN(3) to HN(6) synapse $n=15$, $CV=0.39$ and average= $84.4\text{pA} \pm 33.1\text{pA}$. For the HN(4) to HN(6) synapse $n=16$, $CV=0.41$ and average= $78.3\text{pA} \pm 32.3\text{pA}$. For the HN(3) to HN(7) synapse $n=18$, $CV=0.29$ and average= $70.7\text{pA} \pm 20.6\text{pA}$. For the HN(4) to HN(7) synapse $n=13$, $CV=0.52$ and average= $72\text{pA} \pm 37.5\text{pA}$.

Figure Ten:

The middle premotor interneurons in ganglia 6 and 7 receive an electrical connection from the oscillator interneurons. A complete model of the leech heartbeat central pattern generator assumes that these synapses are all of comparable strength (Weaver et al., 2010). A comparison was made within $n=6$ individuals. Each individual is illustrated with a separate icon and each single postsynaptic voltage clamp recording is connected with a solid line.

Figure Eleven:

The HN(6) middle premotor interneurons receive inhibitory input from the HN(5) switch interneuron and electrical input from the HN(3) oscillator interneuron. Graphs illustrate the synaptic strength for n=6 individuals for the HN5 to HN6i and HN3 to HN6 synapse and n=5 individuals for the HN5 to HN7i and HN3 to HN7 synapse. In the HN(6) middle premotor interneurons there is no significant relationship between the electrical and inhibitory connections. In the HN(7) middle premotor interneurons there is a significant relationship between the inhibitory connections and the excitatory electrical connections with a correlation of 0.6. As the inhibitory inputs increase in strength, the excitatory electrical connections also generally increase in strength.

References:

- Boroffka, I. and R. Hamp (1969). "Topographie de Kreislaufsystems und zirkulation bie *Hirudo medicinalis*." Z. Morph Okol Tierre(64): 59-76.
- Bucher, D., A. Prinz and E. Marder (2005). "Animal to animal variability in motor pattern production in adults and During Growth." Journal of Neuroscience **25**(7): 1611-1619.
- Bucher, D., A. Taylor and E. Marder (2006). "Central pattern generating neurons simultaneously express fast an slow rhythmic activities in the stomatogastric ganglion." Journal of Neurophysiology(95): 3617-3632.
- Calabrese, R. (1977). "The Neural Control of Alternate Heartbeat Coordination States in the Leech." J Comp Physiol [A](122): 111-143.
- Dickinson, P. (2006). "Neuromodulation of central pattern generators in invertebrates and vertebrates." Curr Opin Neurobiol. **6**(16): 604-614.
- Edelman, G. and J. Galley (2001). "Degeneracy and complexity in biological systems." PNAS **98**(24): 13763-13768.
- Goaillard, J., A. Taylor, D. Schulz and E. Marder (2009). "Functional consequences of animal-to-animal variation in circuit parameters." Nat Neurosci **12**: 1424-1430.
- Goldman, M., J. Golowasch, E. Marder and L. Abbott (2001). "Global structure, robustness, and modulation of neuronal models." J Neurosci(21): 5229-5238.
- Gramoll, S., J. Schmidt and R. L. Calabrese (1994). "Switching in the activity state of an interneuron that controls coordination of the hearts in the medicinal leech (*Hirudo medicinalis*)." Journal of Experimental Biology **186**: 157-171.
- Grillner, S., H. Markham, E. De Schutter, G. Silberberg and F. LeBeau (2005). "Microcircuits in action -- from CPGs to neocortex." Trends in Neuroscience(28): 525-533.
- Hudson, A. and A. Prinz (2010). "Conductance ratios and cellular identity." PLOS Comput Biol **6**: e 1000838.
- Jezzini, S., A. Hill, P. Kuzyk and R. Calabrese (2004). "Detailed model of intersegmental coordination in the timing network of the leech heartbeat central pattern generator." J Neurophysiol **91**(2): 958-977.
- Katz, P. (1998). "Comparison of extrinsic and intrinsic neuromodulation in two central pattern generator circuits in invertebrates." Exp Physiol. **83**(3): 281-292.
- Kiehn, O., K. Dougherty, M. Hägglund, L. Borgius, A. Talpalar and C. Restrepo (2010). "Probing spinal circuits controlling walking in mammals." Biochem Biophys Res Commun **396**(1): 11-18.
- Krahl, B. and I. Zerbst-Boroffka (1983). "Blood pressure in the leech *Hirudo medicinalis*." Journal of Experimental Biology **107**: 163-168.
- Lund, J. and A. Kolta (2006). "Generation of the central masticatory pattern and its modification by sensory feedback." Dysphagia **21**(3): 167-174.
- Macagno, E. (1980). "Number and distribution of neurons in leech segmental ganglia." J. Comp. Neurol. **190**: 283-302.
- Mamiya, A. and F. Nadim (2005). "Target-specific short-term dynamics are important for the funtion of synapses in an oscillatory network." J Neurophysiol **94**: 2590-2602.
- Maranto, A. and R. Calabrese (1984). "Neural control of the hearts in the leech, *Hirudo medicinalis*. I. Anatomy, electrical coupling, and innervation of the hearts." J Comp Physiol [A] **154**: 367-380.
- Marder, E., D. Bucher, D. Schulz and A. Taylor (2005). "Invertebrate Central Pattern Generation Moves Along." Current Biology **15**: R685-R699.

- Marder, E. and J. Goaillard (2006). "Variability, compensation and homeostasis in neuron and network function." Nature Reviews Neuroscience **7**: 563-574.
- Masino, M. and R. Calabrese (2002). "A functional asymmetry in the Leech Heartbeat Timing Network is revealed by driving the network across various cycle periods." J Neurosci **22**(11): 4418-4427.
- Mentel, T., L. Cangiano, S. Grillner and A. Buschges (2008). "Neuronal substrates for state-dependent changes in coordination between motoneuron pools during fictive locomotion in the lamprey spinal cord." J Neurosci **28**(4): 868-879.
- Norris, B., A. Weaver, L. Morris, A. Wenning, P. Garcia and R. Calabrese (2006). "A central pattern generator producing alternative outputs: temporal pattern of premotor activity." J Neurophysiol **96**(1): 309-326.
- Norris, B., A. Weaver, A. Wenning, P. Garcia and R. Calabrese (2007). "A Central Pattern Generator Producing Alternative Outputs: Pattern, strength and dynamics of premotor synaptic input to leech heart motor neurons." Journal of Neurophysiology.
- Norris, B., A. Wenning, T. Wright and R. Calabrese (2011). "Constancy and Variability in the Output of a Central Pattern Generator." J Neurosci **31**(12): 4663-4674.
- Olsen, O. and R. Calabrese (1996). "Activation of Intrinsic and Synaptic Currents in Leech Heart Interneurons by Realistic Waveforms." J Neurosci **16**(16): 4958-4970.
- Padmanabhan, K. and N. Urban (2010). "Intrinsic biophysical diversity decorrelates neuronal firing while increasing information content." Nat Neurosci **13**: 1276-1282.
- Peterson, E. and R. Calabrese (1982). "Dynamic analysis of a rhythmic neural circuit in the leech *Hirudo medicinalis*." J Neurophysiol **47**(2): 256-271.
- Prinz, A., D. Bucher and E. Marder (2004). "Similar Network Activity from Disparate Circuit Parameters." Nature Neuroscience **7**(12): 1345-1352.
- Rabbah, P. and F. Nadim (2005). "Synaptic dynamics do not determine proper phase of activity in a central pattern generator." J Neurosci **25**(11269-11278).
- Schulz, D., J. Goaillard and E. Marder (2006). "Variable channel expression in identified single and electrically coupled neurons in different animals." Nature Neuroscience **9**: 356-362.
- Schulz, D., J. Goaillard and E. Marder (2007). "Quantitative expression profiling of identified neurons reveals cell-specific constraints on highly variable levels of gene expression." Proceedings of the National Academy of Science USA(104): 13187-13191.
- Selverston, A. (2010). "Invertebrate central pattern generator circuits." Philos Trans R Soc Lond B Biol Sci. **12**(365).
- Siddal, M., P. Trontelj, S. Utevsky, M. Nkamany and K. MacDonald (2007). "Diverse molecular data demonstrate that commercially available medicinal leeches are not *Hirudo medicinalis*." Proc. R. Soc. B **274**(1617): 1481-1487.
- Swensen, A. and B. Bean (2003). "Ionic mechanisms of bursting in dissociated purkinje neurons." J Neurosci(23): 9650-9663.
- Swensen, A. and B. Bean (2005). "Robustness of firing in dissociated purkinje neurons with acute of long-term reductions in sodium conductance." J Neurosci(25): 3509-3520.
- Taylor, A., J. Goaillard and E. Marder (2009). "How Multiple Conductances Determine Electrophysiological Properties in a Multicompartment Model." J Neurosci **29**(17): 5573-5586.
- Thompson, W. and G. Stent (1976a). "Neural control of heartbeat in the medicinal leech. I. Generation of the vascular coordination of heart motor neuron activity by heart interneurons." J Comp Physiol [A] **111**: 261-279.
- Thompson, W. and G. Stent (1976c). "Neuronal control of heartbeat in the medicinal leech. III. Synaptic relations of the heart interneurons." J Comp Physiol [A] **111**: 309-333.

- Tobin, A. and R. Calabrese (2005). "Myomodulin increases Ih and inhibits the NA/K pump to modulate bursting in leech heart interneurons." J Neurophysiol **94**(6): 3938-3950.
- Weaver, A., R. Roffman, B. Norris and R. Calabrese (2010). "A role for compromise: synaptic inhibition and electrical coupling interact to control phasing in the leech heartbeat CpG." Front. Behav. Neurosci **4**: pii. 38.
- Wenning, A., G. Cymbalyuk and R. Calabrese (2004). "Heartbeat control in leeches. I. Constriction pattern and neural modulation of blood pressure in intact animals." J Neurophysiol **91**(1): 382-396.
- Wenning, A. and E. Meyer (2007). "Hemodynamics in the leech: blood flow in two hearts switching between two constriction patterns." Journal of Experimental Biology **210**: 2627-2636.
- Wenning, A., B. Norris, R. Seaman and R. Calabrese (2008). Two Additional Pairs of Premotor Heart Interneurons in the Leech Heartbeat CPG: The More the Merrier
Society for Neuroscience, Washington DC.

Figure One

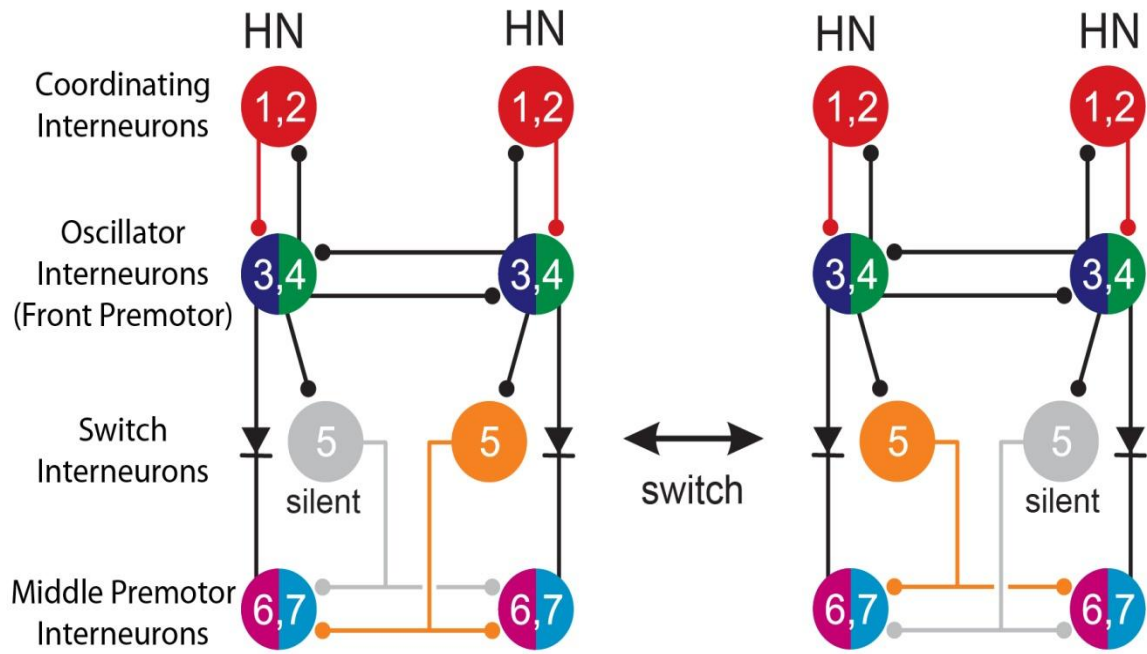


Figure Two

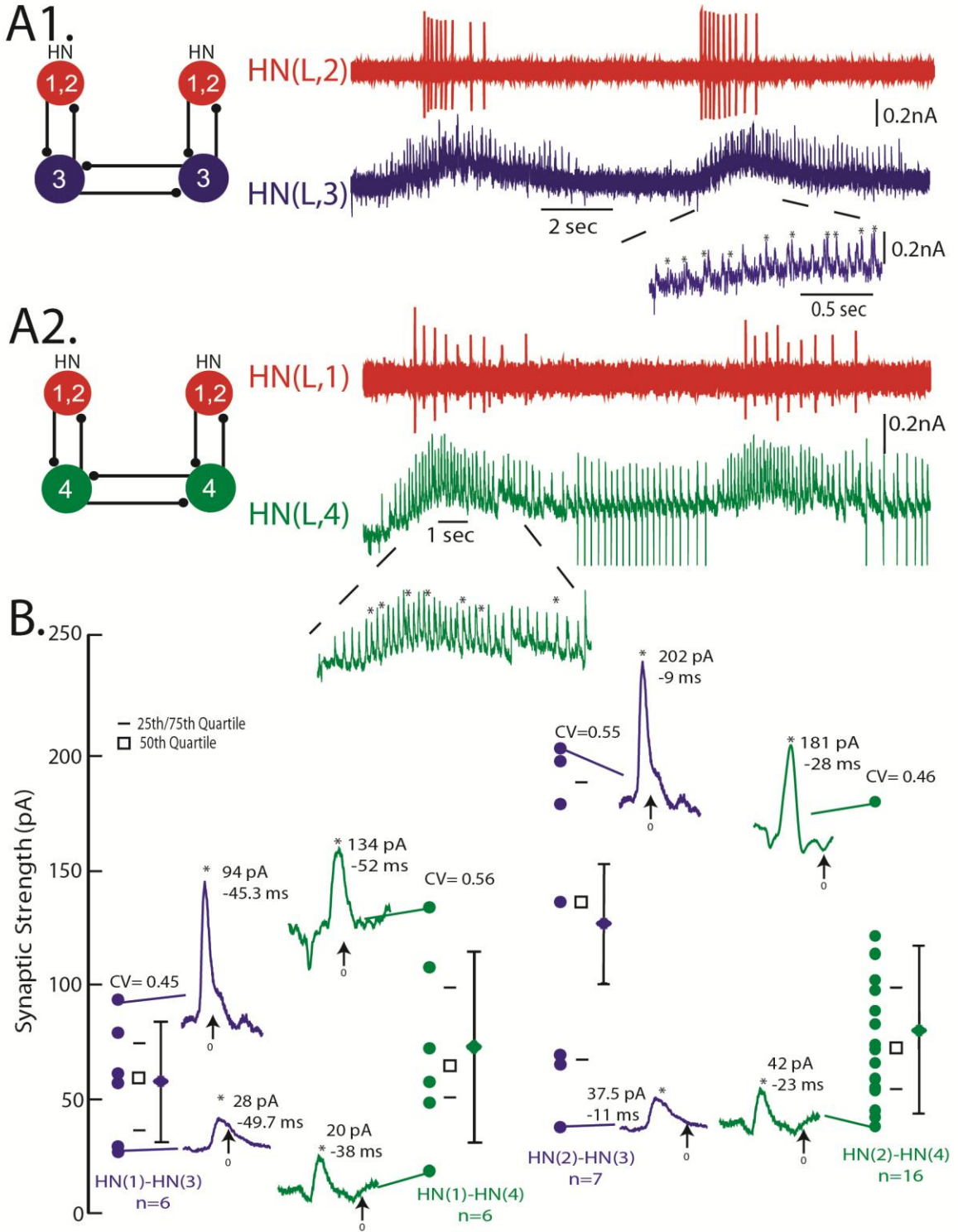
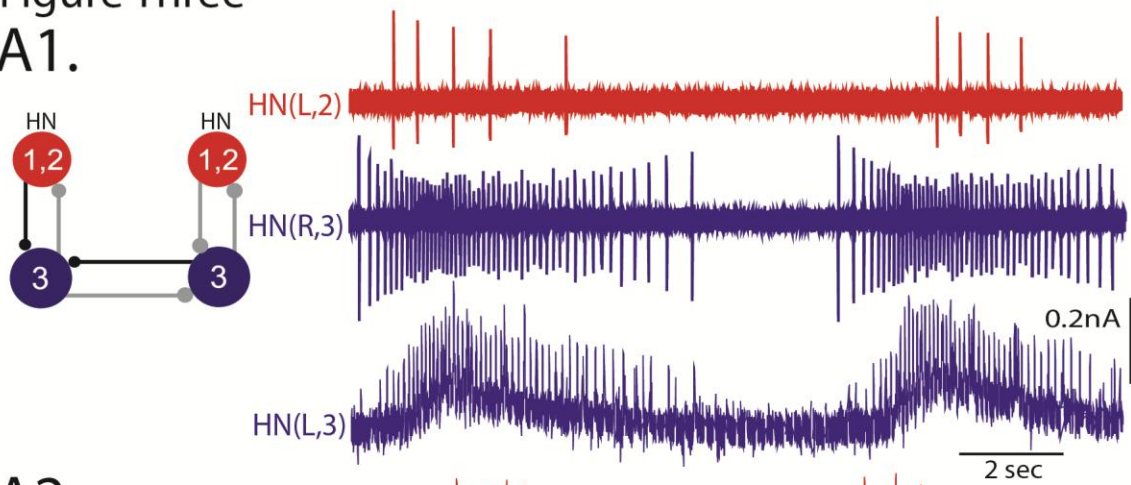
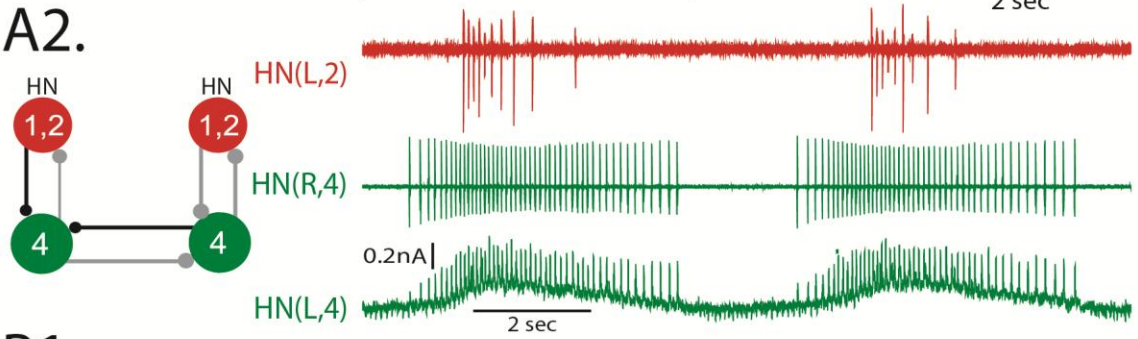


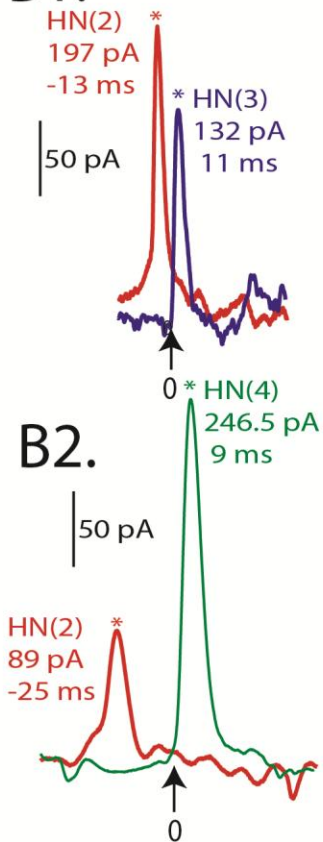
Figure Three
A1.



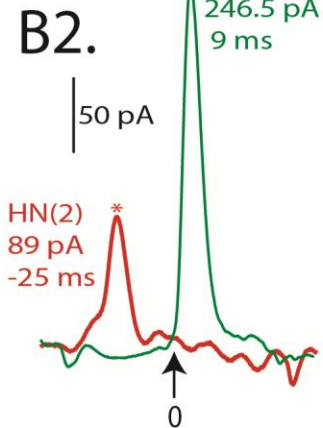
A2.



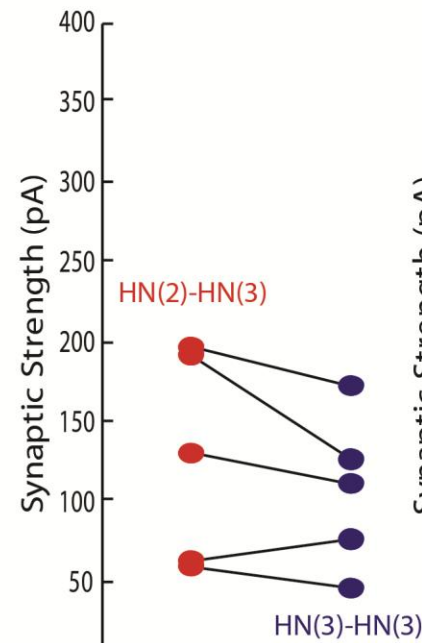
B1.



B2.



C1.



C2.

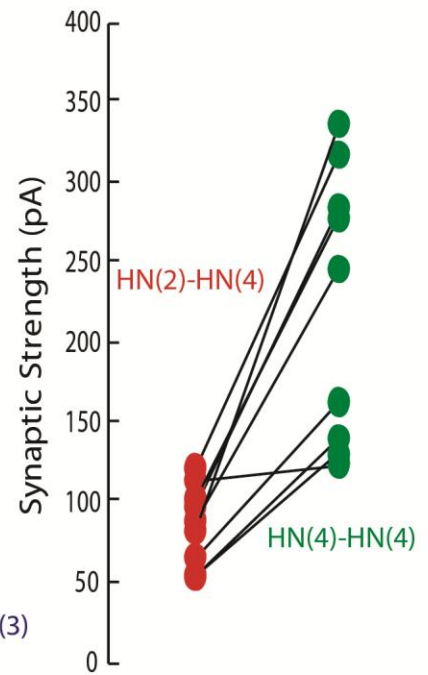


Figure Four

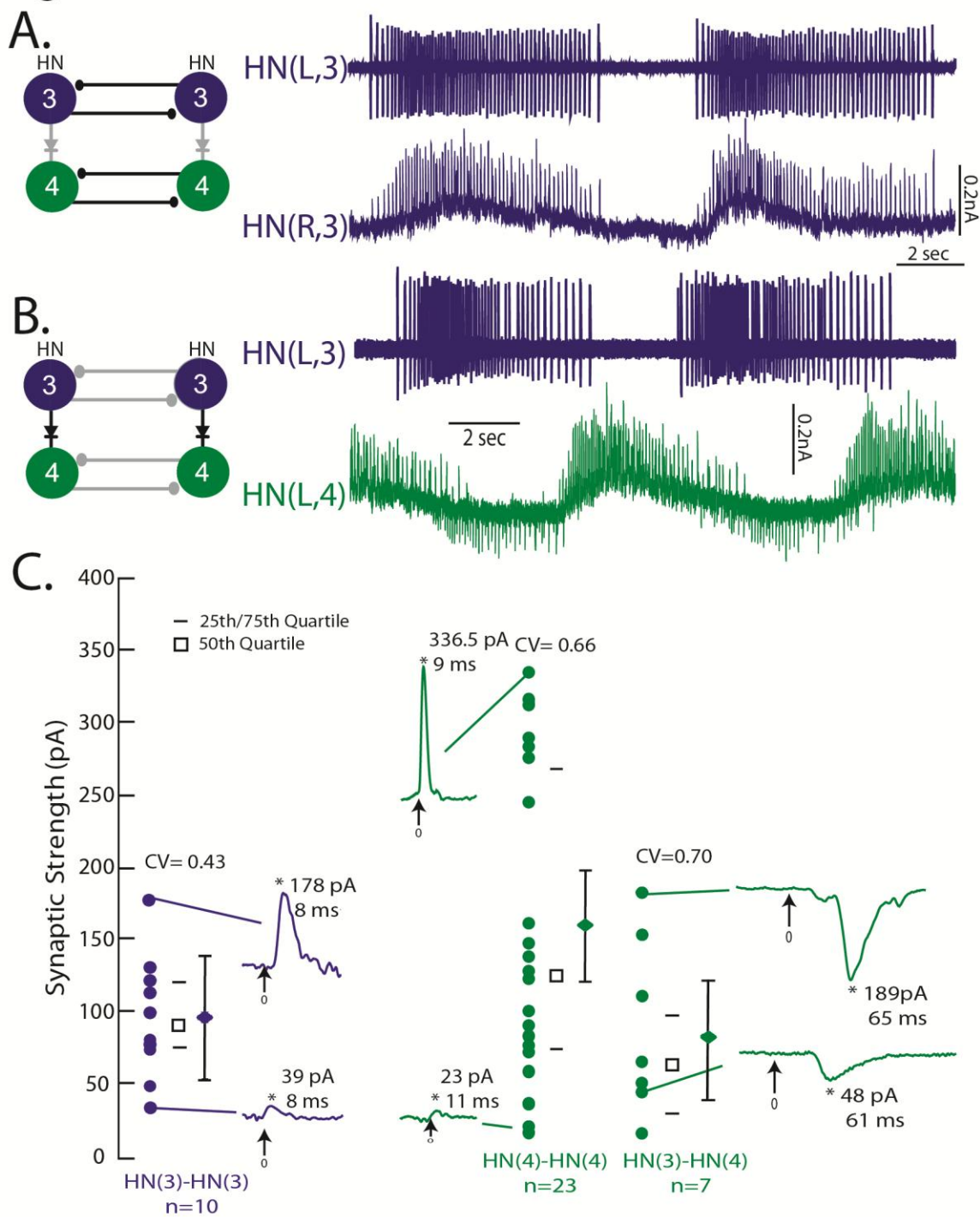


Figure Five

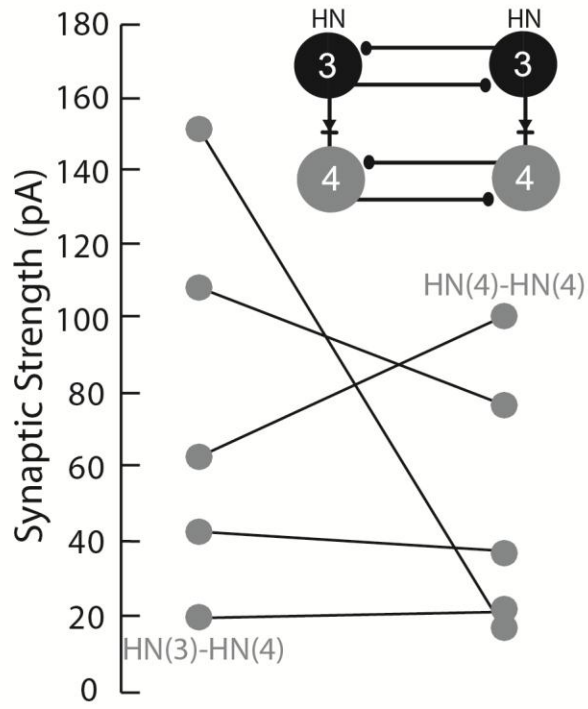
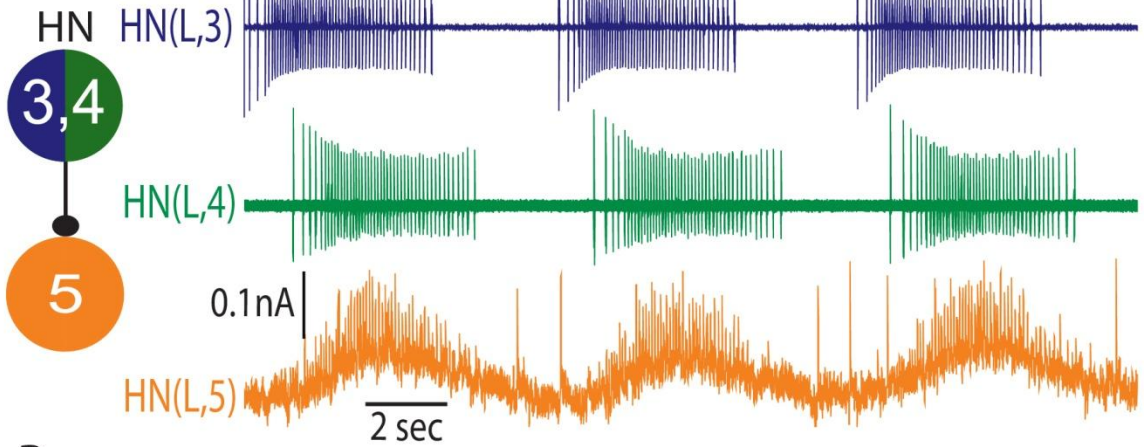


Figure Six

A.



B.

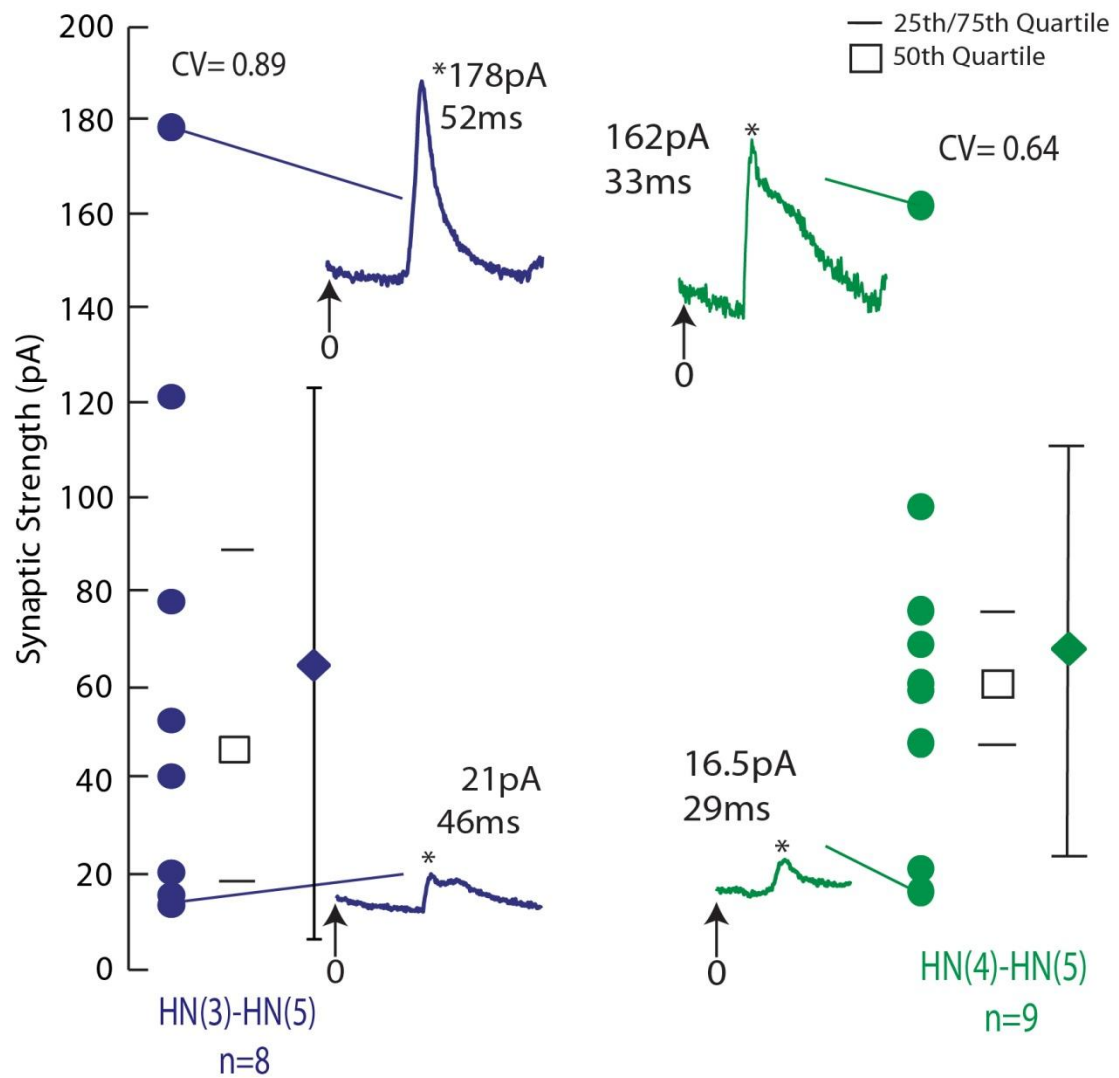


Figure Seven

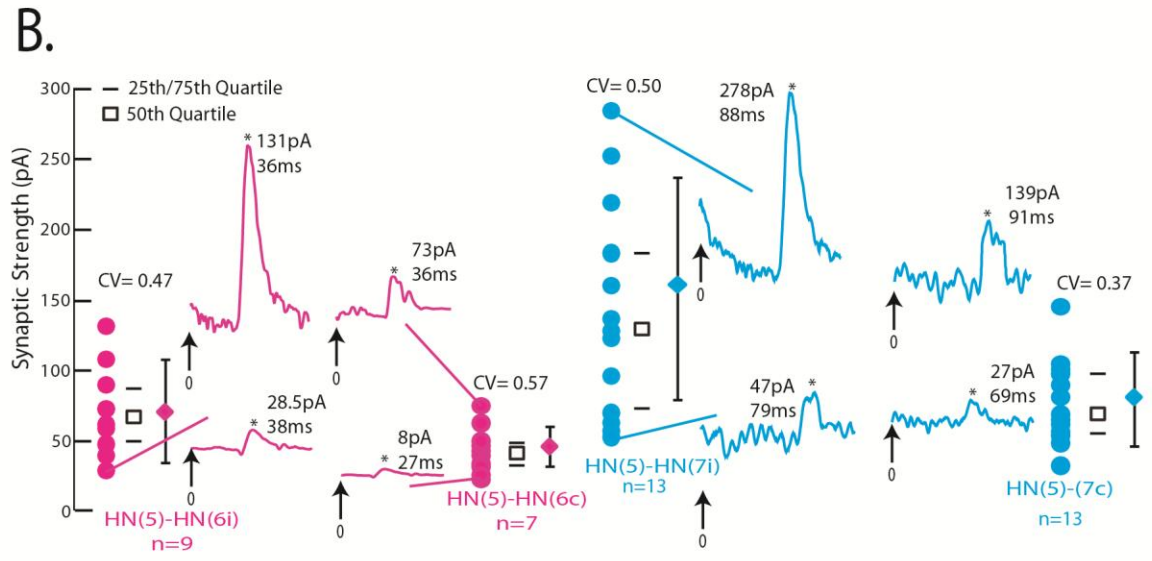
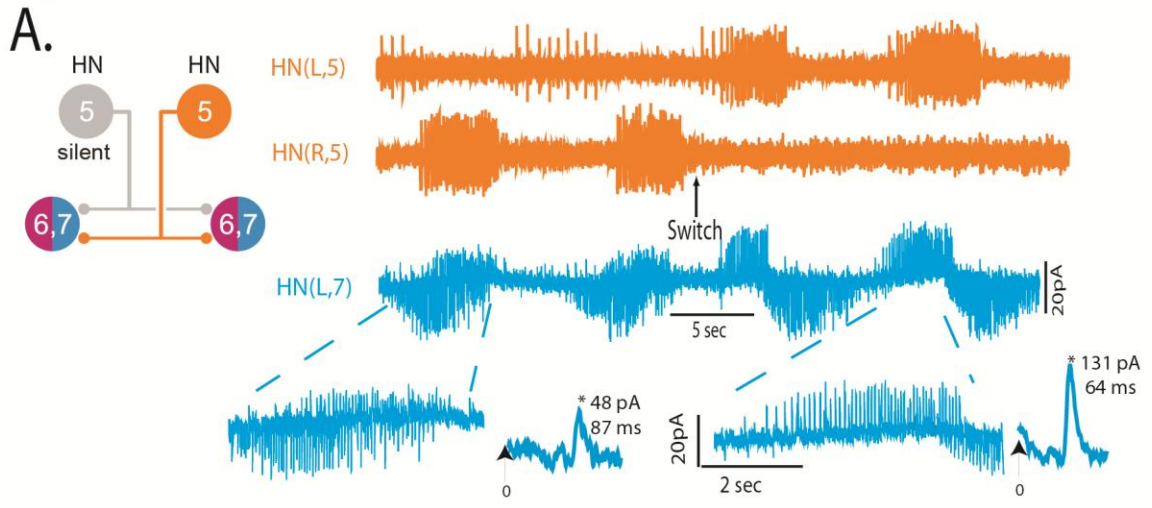


Figure Eight

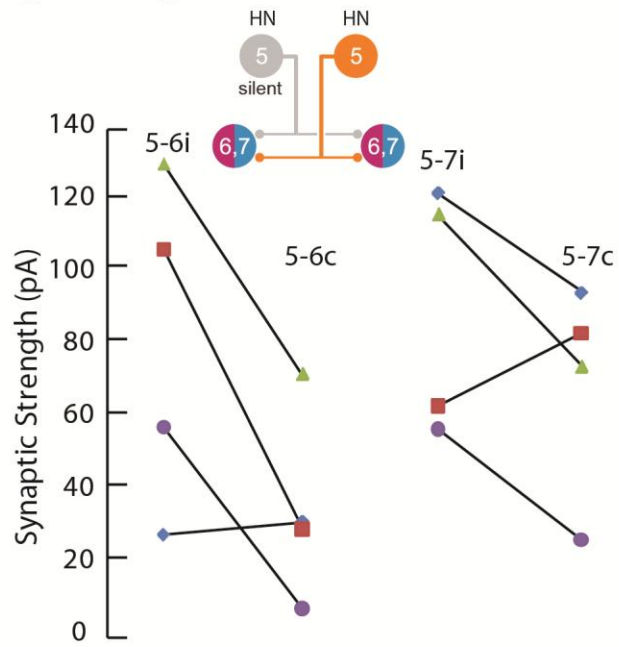
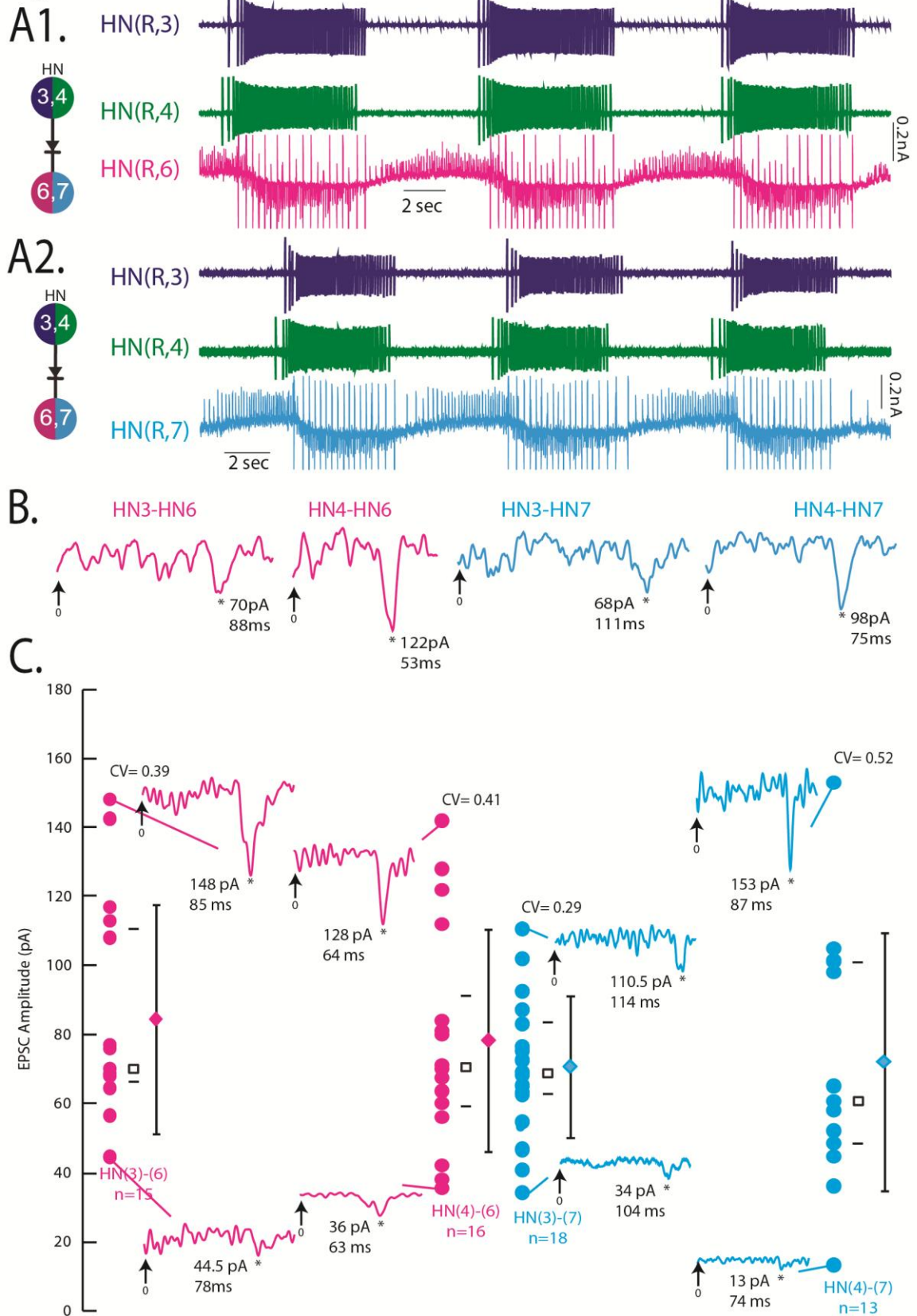


Figure Nine



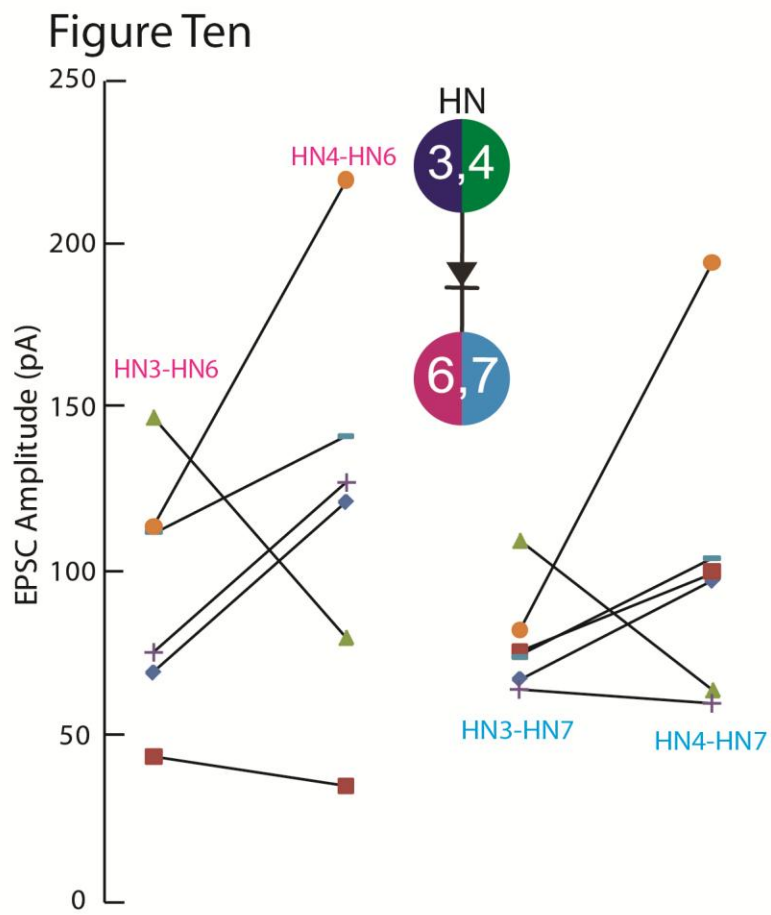


Figure Eleven

